Impact of deforestation on the hydrogen, oxygen and iron isotope compositions of Amazonian streams

Alisson Akerman, Franck Poitrasson, Priscia Oliva, Patrick Seyler, Valmir da Silva Souza, Emmanuel Ponzevera, Roberto Ventura Santos

Stream water evolution following deforestation:

Deforestation

Time

Water Eh, [Fe], $\delta^{57}Fe$:

Water T°C, pH, conductivity, [major cations], [DOC], $\delta^{18}O$, δD:

Impact of deforestation on the hydrogen, oxygen and iron isotope compositions of Amazonian streams.

Alisson Akerman [a,b], Franck Poitrasson [a,b*], Priscia Oliva [a], Patrick Seyler [a,b], Valmir Da Silva Souza [b], Emmanuel Ponzevera [c], Roberto Ventura Santos [b]

[a] *Laboratoire Géosciences Environnement Toulouse, UMR 5563, Centre National de la Recherche Scientifique - Université de Toulouse - Institut de Recherches pour le Développement – Centre National d'Etudes Spatiales, 14-16b, avenue Edouard Belin, 31400 Toulouse, France*

[b] *Instituto de Geociências, Universidade de Brasilia, 70910-900 Brasilia, Brazil*

[c] *Unité Contamination Chimique des Ecosystèmes Marins, IFREMER, Rue de l'Ile d'Yeu, 44311 Nantes, France.*

* Corresponding author.

E-mail address: Franck.Poitrasson@cnrs.fr.

Abstract

We examined the consequences of deforestation and pasture establishment on H, O and Fe isotope cycling in the hydrosphere, with focus on small watersheds from the central and eastern part of Brazilian Amazonia. The $\delta^{18}O$- δD relationships in stream water samples show that the evaporation effect is greater in pasture than in forest, thereby highlighting the impact of deforestation on atmospheric water circulation and rainfall.

A clear effect of deforestation was also found on the dissolved load of these streams. Water temperature, pH, conductivity, major cations and dissolved carbon organic content are lower in forest streams compared to those from deforested areas. Dissolved (i.e., filtrate < 0.45μm) iron concentrations are typically higher in these tropical forest streams. They also show $\delta^{57}Fe$ signatures commonly higher than that of the continental crust (i.e., > 0.1‰). In these black waters enriched in organic matter, the heavier iron isotope composition in the forested areas is related to the oxidized Fe strongly bound to colloidal organic matter. On the other hand, dissolved iron from streams draining older deforested areas shows isotopic compositions usually lighter than the continental crust ($\delta^{57}Fe$ < 0.1‰). The negative $\delta^{57}Fe$ signatures of these areas are likely caused by deforestation involving erosion and rejuvenation of soils in valleys, which leads to the occurrence of a partial iron reduction in the soils. These modifications increased the proportion of isotopically light, dissolved and more reduced Fe in the streams.

Those effects are less obvious on more recent pastures since they display more chemical and isotopic scatter along the sampling months. In a stream flowing through an area undergoing slash and burned deforestation within the year, dissolved iron concentrations and isotopic compositions are much more scattered, with $\delta^{57}Fe$ values varying by >10 ‰ as a result of fire or heavy rain events. This likely depicts the disruption of the iron cycling in the water-soil-plant system with strong changes in the soil mineralogy, organic matter characteristics and biomass activity resulting from the forest fire. Our results suggest that more than a decade is needed to reach a new dynamic steady state of the Fe biogeochemical cycle in pastures.

Hence, the contrasted Fe isotopic compositions between the streams draining pristine tropical forests and those from deforested areas indicate that, like H and O isotopes, Fe isotopes are a sensitive indicator of the transformations affecting the biogeochemical cycling of tropical environment in response to deforestation. However, in contrast to hydrogen and oxygen

isotopes that reveal the exchanges between surface waters and atmosphere, iron isotopes rather highlight the physical-chemical reactions occurring between surface waters and the soils, but with the biomass mediation for all three isotopic tracers.

1. Introduction

The Amazon River Basin drains more than 6 million km^2 representing the main tropical freshwater reserve in the world. It delivers 17% of the riverine freshwater (Callède et al., 2010) and thus large amounts of major and trace elements, including iron, to the open ocean. Therefore, the Amazon River Basin is important to the global carbon and metal nutrient cycles. Previous studies focused on the chemistry of dissolved and particulate loads in natural tropical water revealed the important role of organic colloids on the transport and speciation of metals such as iron in these surface waters (e.g., Benedetti et al., 2002; Benedetti et al., 2003; Eyrolle et al., 1996; Olivie-Lauquet et al., 1999; Olivie-Lauquet et al., 2000; Rose et al., 1998; Viers et al., 1997). A subsequent study by Allard et al. (2002), focused on the suspended solids of the Amazon basin, found that the iron distribution varied with the type of river (i.e., white versus black, the latter showing a larger fraction of trivalent iron complexed with organic matter), suggesting that iron speciation and distribution in the dissolved load also differs depending on the water color. Tropical areas are currently undergoing important modifications due to natural processes such as weathering or podzolization, but also in relation with land use changes involving intensive agricultural practices following deforestation, as reviewed below. We thus need to understand the key role of organic carbon on metal speciation and transport in this context of major geochemical disruption.

The Amazon Forest is the world's largest humid tropical forest (40% of the total rainforests of the world, FAO 2005) extending over 3.65 10^6 km^2. However, each year between

10 and 30 000 km^2 of Brazilian Amazonian forests are converted into agricultural land, mainly pasture. Although deforestation has strongly decreased in the decade following 2004 as a result of public policies and monitoring systems (Nepstad et al., 2014), it is increasing steadily again since 2014 (Fig. 1). Deforestation causes important changes in water balance of Amazonia, with decreases in evapotranspiration and canopy interception. It may affect atmospheric circulation, surface radiation, warming and decreasing rainfall which may lead to severe droughts such as those of 2005 and 2010 (Coe et al., 2013; Eltahir and Bras, 1994; Lewis et al., 2011; McGuffie et al., 1995; Polcher and Laval, 1994; Tinker et al., 1996). As recently reviewed by Akerman et al. (2021), many studies have reported the effects of deforestation associated with the slash-and-burn practice on soil chemical, physical properties and through changes in soil organic matter and biological content, thus affecting the global carbon cycle (e.g., deMoraes et al., 1996; Desjardins et al., 2004; Fearnside and Barbosa, 1998; Fearnside et al., 1993; Fernandes et al., 2002; Fujisaka et al., 1996; Garcia-Oliva et al., 1999; Gibson et al., 2011; Gonzalez-Perez et al., 2004; Khan et al., 2019; Lessa et al., 1996; Neill et al., 1996). On the other hand, only a limited number of studies have reported on the impact of deforestation on the chemistry of surface waters. They focused on the transport of terrigenous organic matter from first order streams to larger rivers in the Amazon Basin (Belanger et al., 2017; Bernardes et al., 2004; de Mello et al., 2018; Farella et al., 2001). Detailed studies by Neill et al. (2001; 2006) suggested that deforestation alter stream hydrology and nutrient concentrations of small stream channels in the Amazon Basin. This for example involved more vegetation on the pasture stream banks along with increased organic matter deposition and storage under riparian grass, and lesser dissolved oxygen with more reduced dissolved iron relative to the forest streams, as will be detailed below.

Iron is mobilized and transferred in complexed and dissolved forms due to different chemical and physical processes (e.g., precipitation, complexation, adsorption, mineral

dissolution, redox processes, chemical weathering, erosion – (Allard et al., 2004; Fritsch et al., 2009; Olivie-Lauquet et al., 1999). Many studies investigated iron isotope fractionation in rivers, lakes and soils (e.g., Bergquist and Boyle, 2006; dos Santos Pinheiro et al., 2014; dos Santos Pinheiro et al., 2013; Emmanuel et al., 2005; Escoube et al., 2009; Fantle and DePaolo, 2004; Ilina et al., 2013; Ingri et al., 2018; Ingri et al., 2006; Li et al., 2017; Mulholland et al., 2015; Poitrasson et al., 2014; Poitrasson et al., 2008; Song et al., 2011; Thompson et al., 2007). These previous works revealed that iron isotope signatures are sensitive tracers of the changes of iron redox, iron speciation/mineral forms or sources in waters and soils. As a result, they provide an additional dimension relative to elemental concentrations to study biogeochemical reactions involving this element, or to determine its sources. This was applied to study continental weathering, riverine element transport, aqueous speciation transformation of iron in different environmental and climatic contexts. However, none of these previous works focused on the effect of deforestation on Fe isotopes in aquatic systems. Yet, deforestation is likely to strongly alter biogeochemical cycles on continental surfaces, including that of iron, through changes in vegetation, of the water cycle, of weathering style and enhanced erosion.

In a previous work, we found that deforestation leaves an imprint on soil Fe isotope compositions. The effect of erosion leads to an isotopic "rejuvenation" towards a lighter soil isotopic composition more akin to that of the continental crust (Akerman et al., 2021). As a result, erosion brings to drainage stream channels isotopically lighter particulate soil-derived matter when compared to forested area remaining untouched. This isotopically lighter material should then become available for subsequent dismantling/dissolution accompanied by a partial iron reduction in soils and streams. From this, we made the prediction that deforestation should lead to lighter dissolved Fe isotope signatures of streams draining deforested areas relative to those draining pristine forests (Akerman et al., 2021). The present work therefore examines the impact of deforestation on the geochemical cycles of key elements, with a focus on iron

123 concentrations and its isotope signature in streams. We compared the dissolved fraction of
124 waters collected in small watersheds from pristine tropical forests with those of watershed
125 draining pastures of different ages established after forest clearing and burning. The main
126 objective of this study was to investigate whether Fe isotopic compositions of dissolved
127 fractions from streams under forest cover and from deforested areas are different and can help
128 us to understand the changes occurring on the Fe cycling after deforestation in a tropical
129 environment.

130 2. Sites description

131 Following the approach of Neill et al. (2001; 2006), we looked for small streams having
132 watersheds either fully located in pristine rainforest, or in pastures of various ages after
133 deforestation to study the biogeochemical effects of deforestation. From this initial survey, we
134 selected two examples: One located in the Para State, near Rio Capim and another one in the
135 Amazonas State, near the city of Presidente Figueiredo (See Akerman et al., 2021, for maps
136 with locations, summarized in Fig. S1).

137 *2.1. The Rio Capim watersheds*

138 We studied one pair of small watersheds (~ 5 km^2), one under "primary" forest cover
139 (without any logging) and another one in a pasture about fifty years old (Akerman et al., 2021),
140 both drained by first order streams. The two watersheds are about 350 km South of the city of
141 Belem, in Eastern Brazilian Amazonia. This study was conducted in the Fazenda Rio Capim
142 owned by CIKEL-Brasil Verde group and located in the district of Paragominas (See Table 1
143 for the GPS coordinates of the study sites).

144 The current regional climate is equatorial with a mean annual rainfall of about 2100 mm
145 (Crepani et al., 2004) and a mean annual temperature and relative humidity of the air are 26.3°C
146 and 81%, respectively (EMBRAPA, 1986). In 2010, the rainfall during the dry season (from

July to November; INMET, see https://mapas.inmet.gov.br/#) was low across Amazonia, comparable to the 2005 drought. Lewis et al. (2011) studied the satellite-derived rainfall data to compare the two major Amazon droughts in 2005 and 2010. This study showed that 57% of Amazonia had low rainfall in 2010 as compared with 37% in 2005. As a result, the streams studied in the present work (Fig. 2) have not flowed throughout the dry season in the year of sampling, hence the lack of results for some of these months on Table 1. Moreover, the next wet season (typically between December to May; INMET) saw a strong stream flooding which destroyed the downstream earth road. Its repair totally modified the hydrology of the stream in generating a pond, and the study site had to be abandoned. Only one more sample was taken from the forest stream in February 2011 (Table 1).

The geomorphology of these watersheds and pedological details of the soils can be found in Akerman et al. (2021). In the riparian zone, the streams drain an albic gleysol in forest and a gleysol in pasture. Semi-deciduous rainforest up to more than 40 meters tall covers 70% of the area. Forest in the cleared basins is commonly converted in Amazonia to pasture by cutting, burning, and planting pasture grasses *Brachiaria brizantha* (Neill et al., 2001).

2.2. The Presidente Figueiredo watersheds

The study was carried out in three watersheds (~ 5 km^2), two of them belonging to the Lake Balbina/Uatumã River watershed, located North of Manaus, near the BR-174 road after the city of Presidente Figueiredo, Central Amazonia, Brazil (See Table 2 for the GPS coordinates of the study sites). One drains a pristine rainforest whereas the two others drain deforested zones.

This area has a hot humid tropical climate, with a mean annual temperature of 26°C, a mean annual air humidity of 85%, and an average rainfall of about 2000 mm per year. The months with maximum rainfall were found from January to May and the dry season extended from August to November (INMET). Considering soils in the riparian zones, one stream

drained an albic gleysol under tropical rainforest that is typical of the region (Guillaumet, 1987), wheras the stream in the slash and burned area drained a gleyic acrisol and the stream from the 12 years old pasture drained a gleysol (Fig. 3). The most recent deforested zone was created from forest clearing and burning in November 2010. The soils of this watershed (Fig. 3b), along with that of the remaining forest (Fig. 3a), corresponding to the Lake Balbina watershed, were studied in detail in Akerman et al. (2021). The stream from an older pasture (Fig. 3c), established 12 years before the study and occurring at the other side, westward from the BR174, in the Rio Pardo watershed, is included in this study. Stream water sample collection was carried out in April 2011 through March 2012, with some gaps essentially corresponding to months when the water was not flowing anymore (Table 2).

3. Sample collection, treatment and chemical analysis

3.1. Sample collection and treatment

Water temperature, pH, conductivity and, for the Presidente Figueiredo sites, Eh, were measured in the field during sampling following methods described in Poitrasson et al., (2014) and Mulholland et al. (2015). Five types of water samples were obtained for each site. After rinsing the filtration system with ~150 ml of stream water, 150 ml of water sample for major elements and alkalinity, 100 ml for trace elements and 500 ml for Fe isotopes were filtered within 6 hours of sampling employing 0.45 μm Millipore membranes (mixed cellulose esters, 47 mm diameter) and preserved in acid-cleaned polyethylene (HDPE) bottles after acidification with double-distilled HNO_3 acid for trace element analysis. Filtered waters for anions, cations, alkalinity and for Fe isotope analysis were not acidified. Moreover, 250 ml of water samples were filtered within 6 hours of sampling through fiberglass filter Whatman GF/F (47 mm diameter) and preserved in acid-cleaned glass tubes after adding ultrapure H_3PO_4 for dissolved

195 organic carbon analysis. Finally, 30 ml of water were also collected, taking care to remove all
196 air bubbles from the sampling bottles for oxygen and hydrogen isotope measurements.

197 *3.2. Elemental analyses*

198 Dissolved total iron and major element (Ca, Mg, Na and K) concentrations of water
199 samples were measured on a quadrupole ICP-MS (inductively coupled plasma mass
200 spectrometry, Agilent 7500, Perkin Elmer) at GET laboratory (Toulouse, France). Indium and
201 rhenium were used as internal standards at ~2-4 ppb. The international geostandards SLRS-4
202 (Riverine Water Reference Material for Trace Metals certified by the National Research
203 Council of Canada) was used to check analytical accuracy and reproducibility. The relative
204 difference between measured concentrations values and the certified data (given for the
205 international geostandard) is less than 5%.
206 The dissolved organic carbon (DOC) was determined also at GET using a *Shimadzu*
207 *TOC-V_{CSN}* analyzer equipped with an autosampler *ASI-V* and software *TOC-Control V*. The
208 measurement uncertainty is about 3% and the detection limit is of 0.1 mg/L.

209 *3.3. Iron isotopes measurements*

210 Aliquots of the filtered solutions, after a multistep dissolution procedure (Poitrasson et
211 al., 2014) using Merck Suprapure reagents (H_2O_2, HF) or bidistilled concentrated acids (HNO_3,
212 HCl), were dried down and redissolved in 0.5 ml of 6 M HCl. The resulting solution was loaded
213 in thermo-retractable Teflon columns and iron was purified using the anionic resin Bio Rad
214 AG1 X4 (200-400 mesh) following the procedure described in Poitrasson et al. (2004). After
215 column chemistry and evaporation, the solutions were redissolved in 0.05 M HCl and stored
216 for iron isotope analyses. Blank tests were performed to estimate the level of contamination
217 induced by the overall dissolution and chemical procedure and was found to be <3-4 ng of Fe.
218 As discussed later, the mineralization and purification procedure were fully duplicated on

219 nearly half of the Presidente Figueiredo samples by a different operator. The so-duplicated
220 isotopic results were undistinguishable within uncertainties and therefore combined together.
221 Most of the iron isotope analyses were performed at the GET laboratory (Toulouse,
222 France), but some samples were analyzed at the IFREMER laboratory (Brest, France) by high
223 and medium mass resolution, using a Neptune Thermo MC-ICP-MS (Multicollector
224 Inductively Coupled Plasma Mass Spectrometry), following the methods described in
225 Poitrasson and Freydier (2005). The measurements included an instrumental mass bias
226 correction using a combination of the "standard-sample bracketing" approach with IRMM-014
227 as the Fe standard, and Ni doping of the purified Fe samples using the daily regression method.
228 The Fe isotope data are reported in the standard delta notation relative to the European
229 reference material IRMM-14, expressed in per mil (‰) for $^{57}Fe/^{54}Fe$ ratio as:

230 $$\delta^{57}Fe = \left(\frac{{}^{57}Fe/{}^{54}Fe_{sample}}{{}^{57}Fe/{}^{54}Fe_{IRMM-14}} - 1 \right) \times 1000$$

231 Data quality was checked by repeated analyses of our in-house hematite standard every 6
232 samples in the analytical sequence. Long-term external reproducibility was estimated from
233 replicate analyses of this hematite in every session, whether using the Sensitive Introduction
234 System or the less stable Apex desolvator as introduction systems to enhance the instrument
235 sensitivity for samples having low Fe contents. Combining the results obtained with both
236 introduction systems, the mean $\delta^{57}Fe$ value of individual measurements for the hematite
237 obtained is 0.761 ± 0.150‰ (2SD, N=81), whereas pooled data by groups of 6 yielded $\delta^{57}Fe$ =
238 0.762 ± 0.068‰ (2SD, N=14). Uncertainties on $\delta^{57}Fe$ and $\delta^{56}Fe$ values reported in this study
239 are expressed as two standard errors (2SE) calculated from the number of replicates and using
240 the Student's t-correcting factor (Platzner, 1997).

3.4. Oxygen and hydrogen isotopes measurements

Oxygen and hydrogen isotope measurements on unfiltered water samples were performed at the University of Brasília after flushing the samples with a mixture of CO_2 + He. After equilibration at 24°C for about 4h, the CO_2 was analyzed for oxygen isotopes using a mass spectrometer Delta V Plus connected to a Gas Bench II inlet system. Hydrogen isotopes were analyzed after high-temperature reaction with CrO_3, using a mass spectrometer Delta V Plus connected to a HDevice inlet system. All analyses are reported in the delta notation relative to the VSMOW international standard (Vienna Standard Mean Ocean Water), expressed in per mil (‰):

$$\delta = \left(\frac{R_{sample}}{R_{VSMOW}} - 1\right) \times 1000$$

where R is the ratio $^{18}O/^{16}O$ or D/H, with δ translating into $\delta^{18}O$ and δD, respectively.

During the analytical sessions, repeated measurements of the international certified reference materials VSMOW, GISP and SLAP from IAEA (International Atomic Energy Agency) yielded differences of ~1‰ for δD and ~0.2‰ for $\delta^{18}O$ compared with the certified values, which is also the estimated long term 2SD reproducibility.

4. Results

4.1. Waters main physical-chemical properties

The studied streams consist of acidic black waters (pH values measured in the field ranging from 4 to 5.5; Table 1 and 2) with little suspended material (i.e., >0.45 μm). In both studied sites, no clear seasonal trends can be seen whatever the considered physical-chemical parameter (Table 1 and Supplementary Fig. S2a, b for streams in the Rio Capim watershed and Table 2 and Supplementary Fig. S3a, b for streams in the Presidente Figueiredo area). However, water temperature, conductivity and pH are systematically lower in the stream

under forest cover for a given sampling month compared to the corresponding deforested areas (Table 1 and 2; Fig. S2a, b and S3a, b). Only the stream draining the recent slash and burned area shows a less systematic relative pH evolution. Conductivity values are low (<20µS/cm), meaning that these rivers are poorly mineralized, with only two exceptions from the pastures and slash and burn at Presidente Figueiredo. The Eh values measured in the Presidente Figueiredo streams range from 315 to 486 mV (Table 2; Fig. S3c). Except for one sample from the slash and burned area, the waters are more oxidized in the stream draining the preserved forest.

Major cation concentrations (Ca, Mg, Na and K; Supplementary Table S1) are generally lower in forest streams compared to those from deforested areas. When comparing sites, we observe that waters from the Presidente Figueiredo area are more diluted than their equivalent from the Rio Capim watershed, except for K. Apart from Ca, rainwaters from the Presidente Figueiredo are also less concentrated in Mg, Na and K than those of the Rio Capim Watershed (Supplementary Table S1).

4.2. Dissolved Organic Carbon concentrations

In the Rio Capim watersheds, waters that drained the albic gleysol in the forest had DOC concentrations ranging from 8.9 to 0.4 mg/kg, whereas waters draining the gleysol in pasture had DOC concentrations ranging from 11 to 1.9 mg/kg (Table 1). For the same sampling date, DOC concentrations are higher in pasture than in forest (Fig. S2b).

Under forest cover in the Presidente Figueiredo watersheds, waters that drained the albic gleysol showed DOC concentrations ranging between 10.5 and 0.42 mg/kg (Table 2). Water samples draining the gleyic acrisol in the slash and burned zone had DOC concentration ranging from 9.5 to 0.33 mg/kg. Finally, a similar range was again measured in the stream waters draining the gleysol from the 12 years old pasture (from 11.1 to 1.16 mg/kg; Table 2). Like the Rio Capim watershed area, DOC concentrations from the stream under forest cover tends to be

289 lower at a given sampling date, but this is not as systematic due to scattered results, both from
290 the slashed and burned area and 12 years old pasture (Fig. S3b).

291 *4.3. Iron concentrations*

292 The two stream waters from the Rio Capim watersheds are characterized by low
293 concentration of total dissolved Fe (i.e., < 83µg/kg, see Table 1). These iron concentrations are
294 systematically higher in forest than in pasture at a given sampling date (Fig. 4a). In contrast to
295 other geochemical parameters, total iron contents of samples collected during the wet season
296 are higher than those obtained during the dry season (Fig. 4a).

297 Water samples that drained the streams of the Presidente Figueiredo watersheds tend to
298 exhibit even lower dissolved Fe concentrations (i.e., ≤ 58µg/kg, see Table 2). However, and as
299 for DOC contents, the relationship is not as systematic as observed for Rio Capim watersheds
300 for the same sampling date: Whereas water samples under forest also show higher Fe
301 concentration in the year 2011, this trend is reversed for two out of the three sampled months
302 of the year 2012 (Fig. 4b).

303 *4.4. Iron isotope compositions*

304 The Fe isotopic composition of the filtered water samples that drained forested and
305 deforested watersheds along the sampling months are given in Table 1 (Rio Capim watersheds)
306 and Table 2 (Presidente Figueiredo watersheds). For the former study site, the water samples
307 collected under forest cover show a heavy δ^{57}Fe signature relative to the continental crust (0.10
308 ± 0.03‰; (Poitrasson, 2006) whereas the water samples collected in pasture are lighter (Fig.
309 5a). No obvious seasonal trend can be seen, however. For the Presidente Figueiredo watersheds,
310 the systematics is more complex (Fig. 5b): Whereas the forested stream water show, with one
311 exception, δ^{57}Fe similar to or higher than the continental crust value, the twelve years old
312 pasture stream, and especially the stream draining the slash and burned area are extremely

scattered since the range observed (>10‰ in $\delta^{57}Fe$, with values going from -7.49±0.33‰ to 3.19±0.09‰; Table 2) is close to the maximum range observed so far at the scale of the Earth (See Ilina et al., 2013; Köster et al., 2023; Rouxel et al., 2008). The possible reasons for these contrasted and extreme results, which were confirmed by a full duplication of the analytical procedures for more than half of the samples (See Table 2), will be discussed below.

4.5. Oxygen and Hydrogen isotope compositions

In the Rio Capim site, $\delta^{18}O$ signatures show little variable values around -4‰ and δD compositions vary between -25.8 and -28.4‰ under forest cover whereas in pasture a large variation is observed ranging from -1.52 to -4.74‰ for $\delta^{18}O$ compositions and from -14.9 to -31.0‰ for δD signatures according to time (Table 3; Fig. 6a).

In the Presidente Figueiredo site, analyses of water samples in forest and cleared and burned zone show little variable oxygen isotope compositions with values varying between -5.82 and -5.27‰ while δD signatures vary between -38.0 and -36.3‰ for the forest watershed and between -36.3 and -35.2‰ for the cleared and burned zone (Table 3; Fig. 6b). The pasture about twelve years old shows $\delta^{18}O$ and δD compositions isotopically heavier, ranging from -5.34 to -4.34‰ and from -32.1 to -27.5‰, respectively (Table 3; Fig. 6b).

Overall, most data plot below the Global Meteoric Water Line (Craig, 1961a; Fig. 6). It thus appears that whatever the watershed, oxygen and hydrogen isotope compositions under forest cover exhibit a narrower variation range and more negative delta isotope values relative to pastures. Samples from Presidente Figueiredo stream that drain slash and burned zone fall between these two extremes, but closer to the forest data (Fig. 6b). In general, the two watersheds of the Rio Capim site present oxygen and hydrogen values isotopically heavier than the watersheds of the Presidente Figueiredo study site (Fig. S4).

5. Discussion

5.1. The $\delta^{18}O$ - δD relationship

When natural water bodies undergo evaporation and/or condensation, hydrogen isotopes are fractionated in proportion to oxygen isotopes. Therefore, H and O isotope distributions are correlated in meteoric waters following the relationship (Craig, 1961b):

$$\delta D = 8 \times \delta^{18}O + 10 \text{ (Global Meteoric Water Line)}$$

This Global Meteoric Water Line (GMWL) has a slope equal to 8 that corresponds to a Rayleigh process at liquid-vapor (local) equilibrium. Its intercept of 10 represents the deuterium excess (Craig, 1961b) which corresponds to the δD when $\delta^{18}O$ equals to zero. However, continental meteoritic waters produced by evaporation of a water body show smaller and variable slopes (typically 5-6), which are usually referred as Local Meteoric Water Line (LMWL). The slope and intercept of the LMWL reflect local climatic conditions that affect water evaporation kinetics in a certain region (Fontes, 1976; Martinelli et al., 1996; Salati et al., 1979). Deviation from the GMWL, which may be defined by the deuterium excess parameter (d-excess), occurs particularly under stronger gradients of relative humidity. Deuterium excess is a second order parameter related to non-equilibrium evaporation conditions (Dansgaard, 1964; Pfahl and Sodemann, 2014). The enrichment of the heavy isotopic species in residual surface waters as a result of the isotopic fractionation that accompanies evaporation was recognized long ago for lakes (Craig, 1961b).

The $\delta^{18}O$ - δD regression for stream waters from the Rio Capim watersheds with the 8 data available, and for those from the Presidente Figueiredo watersheds from the 22 data available (Table 3 and Fig. 6) are given in equation (1) and (2) respectively:

$$\delta D = 4.88(\pm 0.49) \times \delta^{18}O - 6.18(\pm 1.85) \quad \text{(Eq. 1)}$$

$$\delta D = 6.16(\pm 0.37) \times \delta^{18}O - 1.61(\pm 1.99) \quad \text{(Eq. 2)}$$

361 Whereas slopes of these equations are lower than the value of 8 from the Global Meteoric Water
362 Line, their intercept is negative. This deviation from GMWL indicates that these water bodies
363 underwent variable degrees of evaporation, as previously illustrated on lakes (Craig, 1961b;
364 Fontes, 1976; Martinelli et al., 1996), or large rivers, like the Ganges mainstream (Ramesh and
365 Sarin, 1992). This observation is also supported by the local precipitation data in Manaus and
366 Belém that have positive deuterium excess (Martinelli et al., 1996).

367 Samples from Rio Capim watersheds display the largest deviation from the GMWL
368 among all analyzed samples (Figure 6 and Supplementary Fig. S4). In detail, the Rio Capim
369 stream waters $\delta^{18}O$ versus δD regression line (Fig. 6a) shows that the local evaporation effect
370 is stronger in pasture than under forest cover since most stream water data from pasture are
371 heavier than other samples and depart the most from the GMWL. This therefore indicates that
372 deforestation has a major effect on the d-excess quantity, leading to negative values and
373 becoming a "deuterium deficit" relative to the GMWL. These results denote also that
374 evaporation is stronger during the dry season since this effect is even more pronounced in
375 pasture with water samples collected towards the dry season (August 2010) relative to those
376 collected in the middle of the wet season (April 2010; Table 3 and Fig. 6a).

377 The Presidente Figueiredo stream waters data also show a local evaporation effect, but
378 less pronounced deviation from the GMWL if compared to the Rio Capim watersheds (Figs. 6
379 and S4). Evaporation is likewise greater in pasture, which exhibit waters isotopically heavier
380 than those from forest and cleared and burned areas. Samples collected in the wet season
381 (January 2012) have isotopic values close to the GMWL for the three sites studied (Fig. 6b).
382 This result suggests that evaporation is lower during the wet season, even if the water in pasture
383 is enriched in heavy isotopes relative to the water of forest and cleared and burned zone and
384 therefore more subject to evaporation whatever the season.

385 Under forest cover, evaporation effects are weaker because part of the incoming
386 precipitation is intercepted by the canopy and lost by plant transpiration. Exchanges by plant
387 transpiration are quantitatively more important than exchanges by direct evaporation. Such
388 transpiration process does not lead to O and H isotopic fractionation (e.g., Moreira et al., 1997)
389 and the water vapour generated is isotopically similar to the soil water used by the vegetation
390 (Martinelli et al., 1996). In contrast, in the absence of vegetation, evaporation of a free water
391 surface leads to enrichment in heavy H and O isotopes in the remaining liquid, as well as to
392 non-equilibrium conditions of evaporation and, consequently, deviation from the GMWL.
393 Therefore, vapour generated by evaporation of lakes and rivers is isotopically lighter than
394 vapour generated by transpiration. The greater isotopic effect of evaporation in deforested area
395 is caused by decreases of evapotranspiration, canopy interception, and rainfall in proportion to
396 the scale of deforestation creating droughts more intense, such as those of 2005 and 2010 (Coe
397 et al., 2013; Lewis et al., 2011). There is thus a clear $\delta^{18}O$ - δD deforestation signal in
398 Amazonian streams which translates into negative "deuterium excess", previously not found in
399 other Amazonian surface waters (Martinelli et al., 1996).
400 The heavier $\delta^{18}O$ - δD isotope values measured in the Rio Capim site streams compared
401 to the President Figueiredo ones could be explained by a stronger evaporation effect for the
402 former, given notably the older and larger pasture of Rio Capim. However, this observation can
403 also be made for the forest streams (Fig. 6 and S4), which suggests that this could also be due
404 to different LMWL. Although based on meteoric waters older than the sampling dates of the
405 present study, the compilations found on the IAEA repository of GNIP stations
406 (https://nucleus.iaea.org/wiser/explore/) indeed show that whereas rain waters from the Manaus
407 station display a LMWL very close to the GMWL, those of Belem show a LMWL with a slope
408 significantly lower (6.3±0.3) and d-deficit also lower (5.0±0.9). These streams $\delta^{18}O$ - δD
409 isotope data should thus not be interpreted in absolute numbers for deforestation studies, but

rather compare local forested and deforested area. Moreover, the LMWL will also impact these $\delta^{18}O$ - δD values. As another word of caution, negative "d-excess" values are not necessarily strict markers of deforestation since these were also found in the Ganges River mainstem by Ramesh and Sarin (1992) which did not specifically study the effect of deforestation. This does not mean, however, that part the land surface drained by the Ganges River were not partly affected by deforestation.

5.2. Solute dynamics in the Amazonian streams undergoing deforestation

Whatever the studied watersheds, thermodynamic calculations show that all the analyzed stream waters are located on the ferrihydrite stability curve, and are over-saturated relative to goethite and hematite when data are plotted in a log Fe vs pH diagram (Supplementary Fig. S5).

The relationship between Ca/Na and Mg/Na molar ratios for the studied stream waters and rainfall are reported in Table S1 and compared to literature data in Fig. S6. The rainfall chemistry broadly reflects the distance relative to the Atlantic Ocean, with Ca/Na increasing away from the coast (Circles in Fig. S6). This effect is not observed in stream waters however, suggesting that the rain does not directly influence streams chemistry, at least for these major element ratios.

Considering the stream waters themselves, we find that the studied samples collected in different forest sites show distinct values, but they vary little throughout the sampling months (blue diamonds in Fig. S6): Whatever the season (dry or wet) and the study site (forest in the Rio Capim or Presidente Figueiredo watersheds), the chemical signature under forest cover remains the same in a given site for all samples but one. This result suggests that there is a dominating site effect on the chemistry of stream waters draining forest areas. By contrast, whatever the deforested area (pasture of 50 years old or cleared and burned zone), stream water samples are located on a straight line with a slope of 1 (Fig. S6). This alignment is not simply

435 related to the seasons (Table S1), and there is no visible site effect. The straight line shows an
436 equivalent enrichment of Ca and Mg relative to Na. It is therefore difficult to infer an
437 evaporation effect. These results suggest the contribution of a reservoir enriched in Ca and Mg
438 in stream waters from deforested areas relative to those in preserved forests. Further
439 investigations would be required to evaluate whether this is due to a vegetation change effect,
440 mineral weathering resulting from soil rejuvenation following initial erosion or to Ca/Mg-
441 carbonate or sulphate amendment by the farmers.

442 When we compare the results from this study with the literature, we can note similarities
443 and differences. The Ca/Na and Mg/Na ratios of the stream waters from the Capim catchment
444 under forest are close to data from Hieronymus et al. (1993) from the Capim River itself (Fig.
445 S6). Data published by Horbe and Oliveira (2008) on the nearby Coruja and Canoas Rivers are
446 closer to the results obtained in the cleared and burned zone near to Presidente Figueiredo than
447 data measured in the watershed under forest. It is possible that the smaller rivers like Corujas
448 and Canoas are more sensitive to local deforestation than larger rivers like Capim. A full
449 hydrochemical assessment would be required to go further into these comparisons.

450 Williams et al. (1997) also observed an increase of Ca/Na and Mg/Na ratio in a
451 deforested stream compared to the pristine case. However, Neill et al. (2006) observed the
452 opposite and suggested this could result from Na enrichment in pasture stream as a result of
453 cattle feed supplements. Accordingly, Williams et al. (1997) only report manioc plantations in
454 the deforested area, and the slash and burned area of President Figueiredo was deemed for
455 banana and rice plantations, with no cattle present either. On the other hand, some cattle was
456 reported in the Rio Capim site (although we did not see it during our multiple field trips), but it
457 was apparently rare and might not have been Na supplemented.

5.3. Variations of dissolved Fe concentrations and isotopic compositions, organic carbon and Fe/C ratio in waters under forest cover

Whatever the watersheds studied (Rio Capim or Presidente Figueiredo), Fig. 4a and b show that Fe concentrations in stream waters draining forests are generally higher compared to their deforested counterparts sampled at the same time. Moreover, forest stream waters are enriched in heavy Fe isotopes relative to the continental crust (~ 0.10 ± 0.03‰; (Poitrasson, 2006); See Fig. 5a and b). The only notable exception to this rule is sample PF5 F9 sampled in September 2011 (Table 2) when the stream water was no longer flowing. It is thus feasible that some biogeochemical process affected the dissolved Fe isotope signature in this stagnant water body. In contrast, streams from deforested area are mostly lighter (Fig. 5a and b) and tend to show a lower Fe/C ratio (Fig. 7). However, those trends are clearer cut for older, more established pasture (50 years old) relative to younger ones (12 years old and especially the recent slash and burned zone), as will be discussed in more detail in the next section.

Interestingly, above continental crust dissolved Fe isotopic data and elevated Fe/C ratio were also found in the Negro River (dos Santos Pinheiro et al., 2014; Mulholland et al., 2015) and Nsimi Stream (a Mengong River tributary from Cameroon; Akerman et al., 2014) and thus correspond to the stream waters from this study collected in forested area (Fig. 7). The latter thus seem to be similar to dark-coloured tropical waters rich in organic matter from Amazon and Congo basins (Dupre et al., 1996; Olivie-Lauquet et al., 2000). Accordingly, Benedetti et al. (2003) previously uncovered Fe and dissolved organic carbon concentrations leading to variable but similarly high molar ratio of Fe/C in the Negro River. These data thus confirm that the streams under forest cover remain dominant in Amazonia as source for black water rivers like the Negro River. This is also consistent with forest stream water temperatures with values between 25 and 27°C, acid pH ranging from 4 to 5 and conductivity from 4 to 17 µS/cm measured in situ (Table 1 and Table 2) that are close to the characteristics of the Negro River

483 (e.g., Allard et al., 2004; Bergquist and Boyle, 2006; dos Santos Pinheiro et al., 2013; Poitrasson
484 et al., 2014).

485 Akerman et al. (2021) have shown a strong Fe depletion and a heavy isotopic
486 composition of bulk soil under forest cover in the Rio Capim watershed. They suggested that
487 these features are linked to a weathering gradient between top hill and foot slope soil drained
488 by waters. This weathering leads to the loss of isotopically light Fe that is drained together with
489 the particulate fraction in the Negro River, which is isotopically light (dos Santos Pinheiro et
490 al., 2014; dos Santos Pinheiro et al., 2013; Mulholland et al., 2015). This contrasts with the
491 heavy isotopic signature of stream waters dissolved fraction found under forest cover (Fig. 5a
492 and b) that can be explained by soil organic matter humification, and subsequent humic
493 substances-Fe complexation. This results in the presence of metal complexes in solution and
494 other studies of organic-rich waters have shown that the Fe dissolved fraction is isotopically
495 heavy due to Fe complexation with low molecular weight organic molecules or organo-mineral
496 moieties (Ilina et al., 2013; Mulholland et al., 2015; Oleinikova et al., 2019).

497 Fritsch et al. (2009) showed that Fe was transferred to rivers after organic matter
498 complexation and leaching in hydromorphic tropical soils like podzols. In fact, in the presence
499 of abundant dissolved organic matter during weathering processes, Fe becomes mobile either
500 as organo-Fe^{III} complexes or dissolved Fe^{II}. The carbon cycle and iron mobility are controlled
501 by redox conditions. It was found that accumulation of organic matter occurring in
502 hydromorphic environments results in an increase of Fe-bearing mineral weathering. A study
503 of the deforestation effect on biogeochemical characteristics of small Amazonian streams
504 showed that concentration of dissolved Fe^{II} is much lower in forest than in pasture (Neill et al.,
505 2006). Although we did not measure the Fe redox in this study, our Eh measurements in the
506 Presidente Figueiredo forest stream (Table 2) reveal more oxidizing conditions relative to
507 deforested areas and therefore probably more oxidized Fe (with a Fe^{2+}-Fe^{3+} transition near 450-

508 500mV given our forest stream water pH (Table 2), and according to Brookings (1988) and
509 Langmuir (1997) compilations).

510 High level affinity of Fe for organic ligands is well known. Olivié-Lauquet et al. (1999)
511 found that in black waters, over 50% of Fe is associated with organic colloids by complexation.
512 In the particulate fraction of the Negro River, iron speciation is dominated by iron
513 oxyhydroxides (e.g., Allard et al., 2002), whereas it is controlled by the organic matter in the
514 colloidal fractions (Benedetti et al., 2002). Similar results were described in waters that drained
515 small tropical watersheds from central Amazonia where podzolisation processes occur (Eyrolle
516 et al., 1996). A more recent study in podzolic areas has shown that over 80% of Fe is transported
517 in dissolved and colloidal fractions, mainly in the form of organometallic compounds (Patel-
518 Sorrentino et al., 2007). Among the two major organic matter reactive groups occurring in these
519 black waters, Allard et al. (2004) estimated that the contribution of the phenolic group for
520 organo-Fe complexation increases from 33 to 85% when the pH increases in the 4 to 7 range,
521 while the contribution of the carboxylic group decreases from 67 to 15%. Carboxylic acids are
522 assumed to originate from the degradation of polyhydroxyaromatics molecules, as their
523 quantities are highly correlated; This process essentially results from the extensive humification
524 of the degradation products of terrestrial plant (Rose et al., 1998). Water samples that drained
525 forest watershed show pH values lower than in pasture (Table 1, 2 and Fig. S2b and S3b). In
526 this context, this lower pH means that the colloidal Fe is more complexed by carboxylic groups
527 according to the previous works cited above, including Allard et al. (2004), and this strong
528 association with organic matter is more important in forest than in pasture. It is also different
529 relative to the particulate fraction due to different Fe speciation. Although an increasing number
530 of studies relate the Fe speciation with its isotopic composition in organic-rich natural waters
531 (Akerman et al., 2014; Ilina et al., 2013; Oleinikova et al., 2019), a more detailed discussion on
532 this topic would require a careful spectroscopic and Fe isotope study of the same samples as

done by Mulholland et al. (2015) in their study of the Amazon mixing zone. The different proportion of organo-Fe complexation reviewed above suggests likewise that isotope fractionation occurs in organic-rich waters between dissolved Fe and particulate Fe, as previously shown (e.g., Bergquist and Boyle, 2006; Escoube et al., 2009; Mulholland et al., 2015). However, without data on the particulate fraction, it is not possible to elaborate further on the present case study.

5.4. Effect of deforestation on iron isotope signatures

There are some systematic differences between streams from deforested area relative to streams draining preserved forests. Streams from deforested area show heavier O and H isotope composition that depart most from the Global Meteoric Water Line (Fig. 6a and b) because of increased stream water evaporation relative to plant transpiration. These waters also display higher temperature, conductivity (Fig. S2a and S3a), pH, DOC concentrations (Fig. S2b and S3b), major cation concentrations (Table S1) and lower Eh (Table 2 and Fig. S3c). This systematics is more apparent in well-established pasture (50 years old) relative to more recently established ones (12 years old). Notably, the more recently slash and burned area gives particularly scattered results along the sampling months. Following this pattern, Fe concentration is also lower in streams draining deforested area than their pristine counterpart (Fig. 4a and b). Fifty years old pasture stream waters are isotopically lighter (from 0.193 ± 0.081‰ to -0.288 ± 0.081‰) than those from forest and equal to or lower than the average continental crust (Table 1 and Fig. 5a). It has been shown in the studied sites that in addition to chemical weathering, deforestation involves geomorphological modifications by erosion and accumulation of eroded material (Akerman et al., 2021). These geomorphological modifications lead to reductimorphic features in the valley soil profile. Coupled with downhill transport, this leads to rejuvenation of these valley soils. Chemical weathering and erosion

557 processes yield soil Fe isotopic signatures remaining heavier than the continental crust but
558 lighter than the valley soil profile under forest cover (Akerman et al., 2021). These results on
559 the effect of deforestation (Fig. 5a) are consistent with Fantle and DePaolo (2004) suggestion
560 that the net effect of continental weathering is to mobilize small amounts of isotopically light
561 Fe in an exchangeable or dissolved form.

562 Gleysols are representative of wetlands and characterized by reduction processes with
563 or without Fe segregation due to a sufficiently long period of water saturation. These soils are
564 generally related to shallow groundwater leading to a reduction of Fe^{III} to mobile Fe^{II} (Quesada
565 et al., 2011). Several studies have focused on the effect of the change in Fe redox state or the
566 complexation by distinct ligands in aqueous solutions that could induce Fe isotope fractionation
567 (e.g., Bullen et al., 2001; Dideriksen et al., 2008; Escoube et al., 2009; Hill et al., 2010; Johnson
568 et al., 2002; Polyakov and Mineev, 2000; Schauble et al., 2001; Skulan et al., 2002; Teutsch et
569 al., 2005). However, no previous study examined the possible effects this change in Fe redox
570 state has on stream waters Fe isotope signature in a deforestation context. Neill et al. (2006)
571 have shown how change in land use from Amazonian forest to pasture influences streams
572 hydrology and biogeochemistry. They found that small pasture streams showed lower
573 concentrations of dissolved oxygen and higher concentrations of dissolved Fe^{II} relative to
574 streams under forest cover. These results suggest that following deforestation, isotopically light
575 and reduced Fe should be lost by chemical weathering and erosion in soils with the development
576 of redox processes (Akerman et al., 2021). Accordingly, this is what is found in filtrated fraction
577 of stream waters in the form of dissolved iron for the 50 years old pasture (Fig. 5a).

578 This isotopic effect is not yet visible on the younger, 12 years old pasture from the
579 Presidente Figueiredo site, however (Fig. 5b). Two possible explanations may be brought
580 forward: 1) It is possible that the transition of the biogeochemical processes affecting iron in a
581 pasture context were not yet fully established in this younger pasture and/or 2) the watershed

582 of the stream from this PF P3 site is still somewhat affected by a forest type Fe isotope cycling
583 since it is possible that the uppermost end of it starts in the forest visible in the background of
584 Fig. 3c. Whatever the exact explanation, the δ^{57}Fe vs Fe/C relationship of the dissolved load of
585 this stream draining the President Figueiredo 12 years old stream is clearly transitional between
586 forest type signature visible on the forest streams from President Figueiredo and Rio Capim
587 watersheds and the well-established 50 years old pasture (Fig. 7).

588 With the exception of its O-H isotope systematics that is close to that of the
589 corresponding forest stream (Fig. 6b), the stream draining recently slash and burned area
590 displays other physico-chemical parameters that deviate less systematically from forest stream
591 values as the 50 years old pasture stream does. Examples of this include pH, DOC content or
592 Fe concentration, as reported above. But the most extreme signal scatter in this slash and burned
593 area is visible with Fe isotope signatures that deviate by a huge amount of more than 10‰
594 (Table 2 and Fig. 5b). The exact mechanisms remain to be established as they likely involve a
595 succession of processes and reactions, but these isotopic variations seem sensitive to rain events
596 (that was noted during the April 2011 sampling, and that corresponded to a very strong storm
597 during the February 2012 sampling) or fire (a new fire was set in December 2011, before the
598 January 2012 sampling). This shows that deforestation by fire completely disrupt the Fe cycle,
599 as expected from the effect of fire on soil minerals, organic matter and biomass that are all
600 involved in this Fe cycling. As a result, it appears that the Fe isotope signature of the dissolved
601 load of streams is a very sensitive indicator of the perturbation of biogeochemical cycles
602 following forest fires. Subsequently, young pastures (12 years old) tend to resume to forest
603 signature (Fig. 5b) before the Fe cycle reaches a new steady state with a lower than continental
604 crust δ^{57}Fe signatures, as found in the 50 years old pasture (Fig. 5a).

605 Neill et al. (2006) also showed that the physical structure of the stream channel is
606 affected by deforestation. Forest stream channels are lined with sandy banks and are

607 characterized by the lack of vegetation, whereas pasture stream channels were bordered by
608 *Brachiaria brizantha* (Neill et al., 2001) implying a higher organic matter loading in pasture
609 streams. Deforestation is characterized likewise by a change in the vegetation Fe metabolism.
610 Grassy vegetation is representative of pasture landscape and is characterized by strategy II
611 plants Fe metabolism. A pioneering study (Guelke and von Blanckenburg, 2007) suggest that
612 strategy I plants, present in the forest, will have a light Fe isotope composition whereas strategy
613 II plants absorb practically unfractionated Fe relative to bulk iron in soils through siderophore
614 complexation. These experiments were conducted under Fe-limiting conditions however and
615 subsequent studies by Kiczka et al. (2010) and Guelke-Stelling and von Blanckenburg (2012)
616 showed that strategy II plants can also reduce soil-available Fe and thus produce shoot and
617 leaves isotopically light. Those mechanisms are well backed by what we know on plant
618 physiology and biochemistry (See review in Wu et al., 2019). Moreover, Akerman et al. (2014)
619 showed that under a tropical context (Cameroon) comparable to the present study, plant leaves
620 and litter are isotopically lighter during the wet productive season relative to the dry,
621 physiologically more quiescent season. Moreover, Fe isotope fractionation could also occur
622 between organo-Fe^{III} complexes in particulate fraction resulting from plant degradation and
623 dissolved Fe^{II} in filtrates. Given the apparent potential role of the vegetation on the isotope
624 composition of Fe found in stream waters, the specific study of Fe isotope in strategy I and
625 strategy II plants representatives of forests and pastures, respectively, will have to be assessed
626 directly in the studied sites.

627 ## 6. Conclusion

628 Dissolved iron in tropical forest stream water samples exhibits a heavy Fe composition.
629 These isotopic results can be explained by the nature and role of organic matter in the
630 weathering of minerals and the transfer of metal ions to rivers of tropical, organic-rich black

631 waters similar to those found in the Amazon and Congo River Basins. This may be due to the
632 accumulation of organic matter in podzolic areas that increases weathering of Fe-bearing
633 minerals and therefore leads to Fe release in solution. The high-level affinity of Fe for organic
634 ligands in the colloidal fraction also plays a major role in the transfer of Fe as organo-Fe^{III}
635 complexes form that becomes mobile and is isotopically heavy.

636 On the other hand, dissolved Fe from stream water samples collected in established
637 pasture are enriched in light Fe isotope. This can be interpreted by geomorphological
638 modifications induced by erosion processes, accumulation of eroded material and rejuvenation
639 of soils drained by streams in valley after deforestation. These modifications give rise to the
640 appearance of redox processes with reductimorphic features. The different redox state of Fe
641 also corresponds to contrasted Fe isotope partitioning that can explain the light Fe signature of
642 of the more reduced dissolved iron in these waters. Furthermore, modification of vegetation
643 and Fe metabolism after deforestation resulting in the change of Fe acquisition strategy of plants
644 (from strategy I representative of forest to strategy II representative of pasture) could also
645 induce Fe isotopic fractionation in stream waters. Streams flowing through younger pasture and
646 recently slashed and burned area however show that it takes more than a decade to reach a new
647 steady state in the iron cycling in these systems. This results from the strong disruption of
648 biogeochemical cycles due to forest fires that is very well revealed by extreme stream water
649 dissolved Fe isotope variations of >10‰ within a year, as seen from monthly sampling.

650 Stable iron isotopes therefore appear to be sensitive geochemical tracers to identify and
651 quantify the importance of organic matter in organometallic complexation and redox processes
652 in the exchanges of Fe at the soil/surface water interface under forest cover or pasture after
653 deforestation. Hence, this first study opens the way through which Fe isotopes may be used as
654 a powerful tool to better understand the impact of deforestation on the biogeochemical cycling
655 of iron in small tropical watersheds. As such, it provides a complementary view relative to H

and O isotopes that clearly denote the effect of deforestation on the water cycle through enhanced water evaporation of more open stream water bodies due to reduced tree cover. Even though this study demonstrates the Fe isotopes sensitivity to deforestation at the stream waters-scale, it has yet to be evaluated how this signal is transferred at a larger scale on the black water rivers from the Amazon Basin.

Acknowledgements

The CIKEL-Brasil Verde group and the IFT (Instituto Floresta Tropical) are thanked for their permission to work on their Rio Capim watershed, their hospitality and their assistance during the sampling campaigns. We also thank Joao from Presidente Figueiredo for his help and hospitality. We thank the technical and engineering staff of GET and UnB Barbara Alcantara Lima, Philippe Besson, Carole Causserand, Jérôme Chmeleff, Camille Duquenoy, Pascal Fraisy, Manuel Henry, Aurélie Lanzanova, Luiz Mancini, Jonathan Prunier and Jeane Grasyelle Silva Chaves for their assistance. This manuscript benefited from two detailed and insightful anonymous journal reviews. AA acknowledges CNRS and CNPq for her PhD grant. This research was partly funded by IRD, ATUPS and co-tutelle PhD support from Université Paul Sabatier, a CAPES-COFECUB Brazil-French exchange program (Te675/10) and through an EC2CO grant, all to FP.

References

Akerman, A., Oliva, P., Poitrasson, F., Boaventura, G.R., Souza, V.D., Seyler, P., 2021. Impact of deforestation on soil iron chemistry and isotope signatures in Amazonia. Chemical Geology, 577(120048): 14.

Akerman, A., Poitrasson, F., Oliva, P., Audry, S., Prunier, J., Braun, J.J., 2014. Isotopic fingerprint of Fe cycling in an equatorial soil-plant-water system: The Nsimi watershed, South Cameroon. Chemical Geology, 385: 104-116.

682 Allard, T., Menguy, N., Salomon, J., Calligaro, T., Weber, T., Calas, G., Benedetti, M.F., 2004.
683 Revealing forms of iron in river-borne material from major tropical rivers of the
684 Amazon Basin (Brazil). Geochimica Et Cosmochimica Acta, 68(14): 3079-3094.
685 Allard, T., Ponthieu, M., Weber, T., Filizola, N., Guyot, J.L., Benedetti, M., 2002. Nature and
686 properties of suspended solids in the Amazon Basin. Bulletin De La Societe
687 Geologique De France, 173(1): 67-75.
688 Belanger, E., Lucotte, M., Moingt, M., Paquet, S., Oestreicher, J., Rozon, C., 2017. Altered
689 nature of terrestrial organic matter transferred to aquatic systems following
690 deforestation in the Amazon. Applied Geochemistry, 87: 136-145.
691 Benedetti, M., Ranville, J.F., Ponthieu, M., Pinheiro, J.P., 2002. Field-flow fractionation
692 characterization and binding properties of particulate and colloidal organic
693 matter from the Rio Amazon and Rio Negro. Organic Geochemistry, 33(3): 269-
694 279.
695 Benedetti, M.F., Mounier, S., Filizola, N., Benaim, J., Seyler, P., 2003. Carbon and metal
696 concentrations, size distributions and fluxes in major rivers of the Amazon basin.
697 Hydrological Processes, 17(7): 1363-1377.
698 Bergquist, B.A., Boyle, E.A., 2006. Iron isotopes in the Amazon River system: Weathering
699 and transport signatures. Earth and Planetary Science Letters, 248(1-2): 54-68.
700 Bernardes, M.C., Martinelli, L.A., Krusche, A.V., Gudeman, J., Moreira, M., Victoria, R.L.,
701 Ometto, J., Ballester, M.V.R., Aufdenkampe, A.K., Richey, J.E., Hedges, J.I., 2004.
702 Riverine organic matter composition as a function of land use changes, Southwest
703 Amazon. Ecological Applications, 14(4): S263-S279.
704 Brookins, D.G., 1988. Eh-pH diagrams for geochemistry. Springer, Berlin, 176 pp.
705 Bullen, T.D., White, A.F., Childs, C.W., Vivit, D.V., Schultz, M.S., 2001. Demonstration of
706 significant abiotic iron isotope fractionation in nature. Geology, 29: 699-702.
707 Callède, J., Cochoneau, G., Ronchail, J., Vieira Alves, F., Guyot, J.L., Guimaraes, V.S., De
708 Oliveira, E., 2010. Les apports en eau de l'Amazone à l'Océan Atlantique. Revue
709 des Sciences de l'Eau, 23(3): 247-273.
710 Coe, M.T., Marthews, T.R., Costa, M.H., Galbraith, D.R., Greenglass, N.L., Imbuzeiro, H.M.A.,
711 Levine, N.M., Malhi, Y., Moorcroft, P.R., Muza, M.N., Powell, T.L., Saleska, S.R.,
712 Solorzano, L.A., Wang, J.F., 2013. Deforestation and climate feedbacks threaten
713 the ecological integrity of south-southeastern Amazonia. Philosophical
714 Transactions of the Royal Society B-Biological Sciences, 368(1619).
715 Craig, H., 1961a. Isotopic variations in meteoric waters. Science, 133(346): 1702-1708.
716 Craig, H., 1961b. Standard for reporting concentrations of deuterium and oxygen-18 in
717 natural waters. Science, 133(346): 1833-&.
718 Crepani, E., Medeiros, J.S., Palmeira, A.F., 2004. Intensidade pluviométrica: uma maneira
719 de tratar dados pluviométricos para análise da vulnerabilidade de paisagens à
720 perda de solo, INPE, São José dos Campos.
721 Dansgaard, W., 1964. Stable isotope in precipitation. Tellus, 16: 436-468.
722 de Mello, K., Valente, R.A., Randhir, T.O., Vettorazzi, C.A., 2018. Impacts of tropical forest
723 cover on water quality in agricultural watersheds in southeastern Brazil.
724 Ecological Indicators, 93: 1293-1301.
725 deMoraes, J.F.L., Volkoff, B., Cerri, C.C., Bernoux, M., 1996. Soil properties under Amazon
726 forest and changes due to pasture installation in Rondonia, Brazil. Geoderma,
727 70(1): 63-81.
728 Desjardins, T., Barros, E., Sarrazin, M., Girardin, C., Mariotti, A., 2004. Effects of forest
729 conversion to pasture on soil carbon content and dynamics in Brazilian
730 Amazonia. Agriculture Ecosystems & Environment, 103(2): 365-373.

731 Dideriksen, K., Baker, J.A., Stipp, S.L.S., 2008. Equilibrium Fe isotope fractionation
732 between inorganic aqueous Fe(III) and the siderophore complex, Fe(III)-
733 desferrioxamine B (vol 269, pg 280, 2008). Earth and Planetary Science Letters,
734 272(3-4): 758-758.
735 dos Santos Pinheiro, G.M., Poitrasson, F., Sondag, F., Cochonneau, G., Vieira, L.C., 2014.
736 Contrasting iron isotopic composition in river suspended matter: The Negro and
737 the Amazon annual river cycles. Earth and Planetary Science Letters, 394: 168-
738 178.
739 dos Santos Pinheiro, G.M., Poitrasson, F., Sondag, F., Vieira, L.C., Pimentel, M.M., 2013.
740 Iron isotope composition of the suspended matter along depth and lateral
741 profiles in the Amazon River and its tributaries. Journal of South American Earth
742 Sciences, 44: 35-44.
743 Dupre, B., Gaillardet, J., Rousseau, D., Allegre, C.J., 1996. Major and trace elements of
744 river-borne material: The Congo Basin. Geochimica et Cosmochimica Acta, 60(8):
745 1301-1321.
746 Eltahir, E.A.B., Bras, R.L., 1994. Sensitivity of regional climate to deforestation in the
747 Amazon Basin. Advances in Water Resources, 17(1-2): 101-115.
748 EMBRAPA, 1986. Normais climatológicas de Paragominas no período de 1980 a 1988,
749 Centro de Pesquisa Agropecuária do Trópico Úmido, Laboratório de climatologia,
750 Belem.
751 Emmanuel, S., Erel, Y., Matthews, A., Teutsch, N., 2005. A preliminary mixing model for
752 Fe isotopes in soils. Chemical Geology, 222(1-2): 23-34.
753 Escoube, R., Rouxel, O.J., Sholkovitz, E., Donard, O.F.X., 2009. Iron isotope systematics in
754 estuaries: The case of North River, Massachusetts (USA). Geochimica et
755 Cosmochimica Acta, 73(14): 4045-4059.
756 Eyrolle, F., Benedetti, M.F., Benaim, J.Y., Fevrier, D., 1996. The distributions of colloidal
757 and dissolved organic carbon, major elements, and trace elements in small
758 tropical catchments. Geochimica Et Cosmochimica Acta, 60(19): 3643-3656.
759 Fantle, M.S., DePaolo, D.J., 2004. Iron isotopic fractionation during continental
760 weathering. Earth and Planetary Science Letters, 228: 547-562.
761 Farella, N., Lucotte, M., Louchouarn, P., Roulet, M., 2001. Deforestation modifying
762 terrestrial organic transport in the Rio Tapajos, Brazilian Amazon. Organic
763 Geochemistry, 32(12): 1443-1458.
764 Fearnside, P.M., Barbosa, R.I., 1998. Soil carbon changes from conversion of forest to
765 pasture in Brazilian Amazonia. Forest Ecology and Management, 108(1-2): 147-
766 166.
767 Fearnside, P.M., Leal, N., Fernandes, F.M., 1993. Rain-forest burning and the global
768 carbon budget - Biomass, combustion efficiency, and charcoal formation in the
769 Brazilian Amazon. Journal of Geophysical Research-Atmospheres, 98(D9):
770 16733-16743.
771 Fernandes, S.A.P., Bernoux, M., Cerri, C.C., Feigl, B.J., Piccolo, M.C., 2002. Seasonal
772 variation of soil chemical properties and CO2 and CH4 fluxes in unfertilized and
773 P-fertilized pastures in an Ultisol of the Brazilian Amazon. Geoderma, 107(3-4):
774 227-241.
775 Fontes, J.C., 1976. Les isotopes du milieu dans les eaux naturelles. La Houille
776 Blanche(3/4): 205-221.
777 Fritsch, E., Allard, T., Benedetti, M.F., Bardy, M., do Nascimento, N.R., Li, Y., Calas, G.,
778 2009. Organic complexation and translocation of ferric iron in podzols of the

779 Negro River watershed. Separation of secondary Fe species from Al species.
780 Geochimica Et Cosmochimica Acta, 73(7): 1813-1825.
781 Fujisaka, S., Bell, W., Thomas, N., Hurtado, L., Crawford, E., 1996. Slash-and-burn
782 agriculture, conversion to pasture, and deforestation in two Brazilian Amazon
783 colonies. Agriculture Ecosystems & Environment, 59(1-2): 115-130.
784 Garcia-Oliva, F., Sanford, R.L., Kelly, E., 1999. Effects of slash-and-burn management on
785 soil aggregate organic C and N in a tropical deciduous forest. Geoderma, 88(1-2):
786 1-12.
787 Gibson, L., Lee, T.M., Koh, L.P., Brook, B.W., Gardner, T.A., Barlow, J., Peres, C.A.,
788 Bradshaw, C.J.A., Laurance, W.F., Lovejoy, T.E., Sodhi, N.S., 2011. Primary forests
789 are irreplaceable for sustaining tropical biodiversity. Nature, 478(7369): 378-+.
790 Gonzalez-Perez, J.A., Gonzalez-Vila, F.J., Almendros, G., Knicker, H., 2004. The effect of
791 fire on soil organic matter - a review. Environment International, 30(6): 855-870.
792 Guelke, M., von Blanckenburg, F., 2007. Fractionation of stable iron isotopes in higher
793 plants. Environmental Science & Technology, 41(6): 1896-1901.
794 Guelke-Stelling, M., von Blanckenburg, F., 2012. Fe isotope fractionation caused by
795 translocation of iron during growth of bean and oat as models of strategy I and II
796 plants. Plant and Soil, 352(1-2): 217-231.
797 Guillaumet, J.L., 1987. Some structural and floristic aspects of the forest. Experientia,
798 43(3): 241-251.
799 Hieronymus, B., Godot, J.M., Boulègue, J., Bariac, T., Négrel, P., Dupré, B., 1993. Chimie du
800 fleuve Tocantins et de rivières côtières de l'est du Para (Brésil), Grands Bassins
801 Fluviaux, Paris, pp. 22-24.
802 Hill, P.S., Schauble, E.A., Young, E.D., 2010. Effects of changing solution chemistry on
803 Fe3+/Fe2+ isotope fractionation in aqueous Fe-Cl solutions. Geochimica Et
804 Cosmochimica Acta, 74(23): 6669-6689.
805 Horbe, A.M.C., Oliveira, L.G.d.S., 2008. Quimica de igarapés de agua preta no nordeste do
806 Amazonas - Brasil. Acta Amazonica, 38(4): 753-760.
807 Ilina, S.M., Poitrasson, F., Lapitskiy, S.A., Alekhin, Y.V., Viers, J., Pokrovsky, O.S., 2013.
808 Extreme iron isotope fractionation between colloids and particles of boreal and
809 temperate organic-rich waters. Geochimica et Cosmochimica Acta, 101: 96-111.
810 Ingri, J., Conrad, S., Lidman, F., Nordblad, F., Engstrom, E., Rodushkin, I., Porcelli, D., 2018.
811 Iron isotope pathways in the boreal landscape: Role of the riparian zone.
812 Geochimica Et Cosmochimica Acta, 239: 49-60.
813 Ingri, J., Malinovsky, D., Rodushkin, I., Baxter, D.C., Widerlund, A., Andersson, P.,
814 Gustafsson, O., Forsling, W., Ohlander, B., 2006. Iron isotope fractionation in river
815 colloidal matter. Earth and Planetary Science Letters, 245(3-4): 792-798.
816 Johnson, C.M., Skulan, J.L., Beard, B.L., Sun, H., Nealson, K.H., Brateman, P.S., 2002.
817 Isotopic fractionation between Fe(III) and Fe(II) in aqueous solutions. Earth and
818 Planetary Science Letters, 195: 141-153.
819 Khan, M.A.W., Bohannan, B.J.M., Nusslein, K., Tiedje, J.M., Tringe, S.G., Parlade, E.,
820 Barberan, A., Rodrigues, J.L.M., 2019. Deforestation impacts network co-
821 occurrence patterns of microbial communities in Amazon soils. Fems
822 Microbiology Ecology, 95(2): 12.
823 Kiczka, M., Wiederhold, J.G., Kraemer, S.M., Bourdon, B., Kretzschmar, R., 2010. Iron
824 Isotope Fractionation during Fe Uptake and Translocation in Alpine Plants.
825 Environmental Science & Technology, 44(16): 6144-6150.
826 Köster, M., Staubwasser, M., Meixner, A., Kasemann, S.A., Manners, H.R., Morono, Y.,
827 Inagaki, F., Heuer, V.B., Kasten, S., Henkel, S., 2023. Uniquely low stable iron

isotopic signatures in deep marine sediments caused by Rayleigh distillation. Scientific Reports, 13(1): 11.
Langmuir, D., 1997. Aqueous environmental geochemistry. Prentice-Hall, Upper Saddle River, 600 pp.
Lessa, A.S.N., Anderson, D.W., Moir, J.O., 1996. Fine root mineralization, soil organic matter and exchangeable cation dynamics in slash and burn agriculture in the semi-arid northeast of Brazil. Agriculture Ecosystems & Environment, 59(3): 191-202.
Lewis, S.L., Brando, P.M., Phillips, O.L., van der Heijden, G.M.F., Nepstad, D., 2011. The 2010 Amazon Drought. Science, 331(6017): 554-554.
Li, M., He, Y.S., Kang, J.T., Yang, X.Y., He, Z.W., Yu, H.M., Huang, F., 2017. Why was iron lost without significant isotope fractionation during the lateritic process in tropical environments? Geoderma, 290: 1-9.
Martinelli, L.A., Victoria, R.L., Sternberg, L.S.L., Ribeiro, A., Moreira, M.Z., 1996. Using stable isotopes to determine sources of evaporated water to the atmosphere in the Amazon basin. Journal of Hydrology, 183(3-4): 191-204.
McGuffie, K., Henderson-Sellers, A., Zhang, H., Durbridge, T.B., Pitman, A.J., 1995. Global climate sensitivity to tropical deforestation. Global and Planetary Change, 10(1-4): 97-128.
Moreira, M.Z., Sternberg, L.D.L., Martinelli, L.A., Victoria, R.L., Barbosa, E.M., Bonates, L.C.M., Nepstad, D.C., 1997. Contribution of transpiration to forest ambient vapour based on isotopic measurements. Global Change Biology, 3(5): 439-450.
Mulholland, D.S., Poitrasson, F., Boaventura, G.R., Allard, T., Vieira, L.C., Santos, R.V., Mancini, L., Seyler, P., 2015. Insights into iron sources and pathways in the Amazon River provided by isotopic and spectroscopic studies. Geochimica et Cosmochimica Acta, 150: 142-159.
Neill, C., Deegan, L.A., Thomas, S.M., Cerri, C.C., 2001. Deforestation for pasture alters nitrogen and phosphorus in small Amazonian Streams. Ecological Applications, 11(6): 1817-1828.
Neill, C., Deegan, L.A., Thomas, S.M., Haupert, C.L., Krusche, A.V., Ballester, V.M., Victoria, R.L., 2006. Deforestation alters the hydraulic and biogeochemical characteristics of small lowland Amazonian streams. Hydrological Processes, 20(12): 2563-2580.
Neill, C., Fry, B., Melillo, J.M., Steudler, P.A., Moraes, J.F.L., Cerri, C.C., 1996. Forest- and pasture-derived carbon contributions to carbon stocks and microbial respiration of tropical pasture soils. Oecologia, 107(1): 113-119.
Nepstad, D., McGrath, D., Stickler, C., Alencar, A., Azevedo, A., Swette, B., Bezerra, T., DiGiano, M., Shimada, J., da Motta, R.S., Armijo, E., Castello, L., Brando, P., Hansen, M.C., McGrath-Horn, M., Carvalho, O., Hess, L., 2014. Slowing Amazon deforestation through public policy and interventions in beef and soy supply chains. Science, 344(6188): 1118-1123.
Oleinikova, O.V., Poitrasson, F., Drozdova, O.Y., Shirokova, L.S., Lapitskiy, S.A., Pokrovsky, O.S., 2019. Iron isotope fractionation during bio- and photodegradation of organoferric colloids in boreal humic waters. Environmental Science & Technology, 53(19): 11183-11194.
Olivie-Lauquet, G., Allard, T., Benedetti, M., Muller, J.P., 1999. Chemical distribution of trivalent iron in riverine material from a tropical ecosystem: A quantitative EPR study. Water Research, 33(11): 2726-2734.

876 Olivie-Lauquet, G., Allard, T., Bertaux, J., Muller, J.P., 2000. Crystal chemistry of
877 suspended matter in a tropical hydrosystem, Nyong basin (Cameroon, Africa).
878 Chemical Geology, 170(1-4): 113-131.
879 Patel-Sorrentino, N., Lucas, Y., Eyrolle, F., Melfi, A.J., 2007. Fe, Al and Si species and
880 organic matter leached off a ferrallitic and podzolic soil system from Central
881 Amazonia. Geoderma, 137(3-4): 444-454.
882 Pfahl, S., Sodemann, H., 2014. What controls deuterium excess in global precipitation?
883 Climate of the Past, 10(2): 771-781.
884 Platzner, I.T., 1997. Modern isotope ratio mass spectrometry. John Wiley & sons,
885 Chichester, 514 pp.
886 Poitrasson, F., 2006. On the iron isotope homogeneity level of the continental crust.
887 Chemical Geology, 235: 195-200.
888 Poitrasson, F., Freydier, R., 2005. Heavy iron isotope composition of granites determined
889 by high resolution MC-ICP-MS. Chemical Geology, 222: 132-147.
890 Poitrasson, F., Halliday, A.N., Lee, D.C., Levasseur, S., Teutsch, N., 2004. Iron isotope
891 differences between Earth, Moon, Mars and Vesta as possible records of
892 contrasted accretion mechanisms. Earth and Planetary Science Letters, 223: 253-
893 266.
894 Poitrasson, F., Vieira, L.C., Seyler, P., dos Santos Pinheiro, G.M., Mulholland, D.S., Bonnet,
895 M.P., Martinez, J.M., Lima, B.A., Boaventura, G.R., Chmeleff, J., Dantas, E., Guyot, J.L.,
896 Mancini, L., Pimentel, M.M., Santos, R.V., Sondag, F., Vauchel, P., 2014. Iron isotope
897 composition of the bulk waters and sediments from the Amazon River Basin.
898 Chemical Geology, 377: 1-11.
899 Poitrasson, F., Viers, J., Martin, F., Braun, J.J., 2008. Limited iron isotope variations in
900 recent lateritic soils from Nsimi, Cameroon: Implications for the global Fe
901 geochemical cycle. Chemical Geology, 253: 54-63.
902 Polcher, J., Laval, K., 1994. The impact of African and Amazonian deforestation on
903 tropical climate. Journal of Hydrology, 155(3-4): 389-405.
904 Polyakov, V.B., Mineev, S.D., 2000. The use of Mössbauer spectroscopy in stable isotope
905 geochemistry. Geochimica et Cosmochimica Acta, 64: 849-865.
906 Quesada, C.A., Lloyd, J., Anderson, L.O., Fyllas, N.M., Schwarz, M., Czimczik, C.I., 2011.
907 Soils of Amazonia with particular reference to the RAINFOR sites. Biogeosciences,
908 8(6): 1415-1440.
909 Ramesh, R., Sarin, M.M., 1992. Stable isotope study of the Ganga (Ganges) river system.
910 Journal of Hydrology, 139(1-4): 49-62.
911 Rose, J., Vilge, A., Olivie-Lauquet, G., Masion, A., Frechou, C., Bottero, J.Y., 1998. Iron
912 speciation in natural organic matter colloids. Colloids and Surfaces a-
913 Physicochemical and Engineering Aspects, 136(1-2): 11-19.
914 Rouxel, O., Sholkovitz, E., Charette, M., Edwards, K.J., 2008. Iron isotope fractionation in
915 subterranean estuaries. Geochimica et Cosmochimica Acta, 72(14): 3413-3430.
916 Salati, E., Dallolio, A., Matsui, E., Gat, J.R., 1979. Recycling of water in the amazon basin -
917 Isotopic study. Water Resources Research, 15(5): 1250-1258.
918 Schauble, E.A., Rossman, G.R., Taylor Jr, H.P., 2001. Theoretical estimates of equilibrium
919 Fe-isotope fractionations from vibrational spectroscopy. Geochimica et
920 Cosmochimica Acta, 65: 2487-2497.
921 Skulan, J.L., Beard, B.L., Johnson, C.M., 2002. Kinetic and equilibrium Fe isotope
922 fractionation between aqueous Fe(III) and hematite. Geochimica et
923 Cosmochimica Acta, 66: 2995-3015.

924 Song, L.T., Liu, C.Q., Wang, Z.L., Zhu, X.K., Teng, Y.G., Liang, L.L., Tang, S.H., Li, J., 2011. Iron
925 isotope fractionation during biogeochemical cycle: Information from suspended
926 particulate matter (SPM) in Aha Lake and its tributaries, Guizhou, China.
927 Chemical Geology, 280(1-2): 170-179.
928 Teutsch, N., von Gunten, U., Porcelli, D., Cirpka, O.A., Halliday, A.N., 2005. Adsorption as a
929 cause for iron isotope fractionation in reduced groundwater. Geochimica Et
930 Cosmochimica Acta, 69(17): 4175-4185.
931 Thompson, A., Ruiz, J., Chadwick, O.A., Titus, M., Chorover, J., 2007. Rayleigh fractionation
932 of iron isotopes during pedogenesis along a climate sequence of Hawaiian basalt.
933 Chemical Geology, 238(1-2): 72-83.
934 Tinker, P.B., Ingram, J.S.I., Struwe, S., 1996. Effects of slash-and-burn agriculture and
935 deforestation on climate change. Agriculture Ecosystems & Environment, 58(1):
936 13-22.
937 Viers, J., Dupre, B., Polve, M., Schott, J., Dandurand, J.L., Braun, J.J., 1997. Chemical
938 weathering in the drainage basin of a tropical watershed (Nsimi-Zoetele site,
939 Cameroon): Comparison between organic-poor and organic-rich waters.
940 Chemical Geology, 140(3-4): 181-206.
941 Williams, M.R., Melack, J.M., 1997. Solute export from forested and partially deforested
942 catchments in the central Amazon. Biogeochemistry, 38(1): 67-102.
943 Wu, B., Amelung, W., Xing, Y., Bol, R., Berns, A.E., 2019. Iron cycling and isotope
944 fractionation in terrestrial ecosystems. Earth-Science Reviews, 190: 323-352.
945
946
947 **Figure captions:**

948

949 Figure 1: Evolution of the annual deforestation in the Amazonian Basin, Brazil. Data
950 source: INPE, program PRODES (www.obt.inpe.br/, access date: 16/06/2023).
951 "Amazonia Legal" was defined by Brazilian law and it covers the 9 states concerned by the
952 Amazon River Basin.

953

954 Figure 2: Photos of the forest (RC F4; a) and 50 years old pasture (RC P3; b) streams
955 studied from the Rio Capim watershed, Para State, Brazil, taken during the wet season
956 (April). The discharges were of 73.4 m^3/h (a) and 12.5 m^3/h (b). The stream flows
957 towards the lower left corner of the picture shown in (b). See Table 1 for more data and
958 Akerman et al. (2021) for more photos of the site.

959

960 Figure 3: Photos of the forest (PF F9; a), slash and burned (PF P6; b) and 12 years old
961 pasture (PF P3; c) streams studied from the Presidente Figueiredo area, Amazonas State,
962 Brazil, taken during the wet season (April). The discharges were of 22 m^3/h (a), 9.2 m^3/h
963 (b) and 12.4 m^3/h (c). See Table 2 for more data and Akerman et al. (2021) for more
964 photos of the site.
965
966 Figure 4: Evolution of dissolved Fe concentrations through the months sampled in the
967 streams from the Rio Capim watershed draining a forest and a 50 years old pasture (a)
968 and in the streams from watersheds near Presidente Figueiredo draining a forest, a
969 slashed and burned area and a 12 years old pasture (b). Data are from Table 1 and 2.
970
971 Figure 5: Evolution of the dissolved iron isotope composition relative to IRMM-14 from
972 streams sampled in the Rio Capim (a) and Presidente Figueiredo (b) watersheds. The
973 mean value of the continental crust (Poitrasson, 2006) is reported for reference. Data are
974 from Table 1 and 2.
975
976 Figure 6: Oxygen and hydrogen isotope composition relative to VSMOW of waters from
977 the streams sampled in the Rio Capim (a) and Presidente Figueiredo (b) watersheds. All
978 samples plot below the Global Meteoric Water Line (GMWL; Craig, 1961a), thus denoting
979 the effect of evaporation. Data are from Table 3.
980
981 Figure 7: δ^{57}Fe relative to IRMM-14 as a function of molar Fe/C ratio in filtered tropical
982 waters from Brazil: Forested and deforested watersheds of Presidente Figueiredo (PF)
983 and Rio Capim (RC), Negro River (dos Santos Pinheiro, 2014; Mulholland et al., 2015), and

984 from Cameroon: Nsimi watershed (Akerman et al., 2014). The mean $\delta^{57}Fe$ value of the
985 continental crust (Poitrasson, 2006) is reported for reference.
986
987 Supplementary Figure S1: General geological map of Brazil showing the locations (stars)
988 of the two studied sites near Belem and Manaus (after Akerman et al., 2021). See Table 1
989 and 2 for the GPS coordinates of the study sites.
990
991 Supplementary Figure S2: Evolution of temperature and conductivity (a), pH and DOC
992 contents (b) through the months sampled in the streams from the Rio Capim watershed
993 draining a forest and a 50 years old pasture. Data are from Table 1.
994
995 Supplementary Figure S3: Evolution of temperature and conductivity (a), pH and DOC
996 contents (b) and Eh (c) through the months sampled in the streams from watersheds near
997 Presidente Figueiredo draining a forest, a slashed and burned area and a 12 years old
998 pasture. Data are from Table 2.
999
1000 Supplementary Figure S4: Oxygen and hydrogen isotope composition relative to VSMOW
1001 of waters from the streams sampled in the Rio Capim and Presidente Figueiredo
1002 watersheds. Most samples plot below the Global Meteoric Water Line (GMWL; Craig,
1003 1961a), thus denoting the effect of evaporation. Note also that the Local Water Line from
1004 Presidente Figueiredo watersheds (eq. 1, see text and Fig. 6b) seem to accommodate well
1005 all data including those from Rio Capim watershed. This may suggest that the local water
1006 line from the Rio Capim watershed is less well defined due to a more limited number of
1007 measurements. Data are from Table 3.
1008

Supplementary Figure S5: Plot of Log Fe_T vs. pH showing all the streamwaters from the Rio Capim and Presidente Figueiredo watersheds. The domain of ferrihydrite stability is obtained by two studies (full line by Diakonov et al., 1994; dotted line by Sigg et al., 2000). The domains of goethite and hematite stability are from Diakonov et al., 1994).

Supplementary Figure S6: Mixing diagram Mg/Na vs. Ca/Na of the dissolved load comparing the data from the present study (RC and PF) to the data from Williams et al. (1997) in Central Amazon, from Hieronymus et al. (1993) in Rio Capim River, from Gaillardet et al. (1997) in Amazon black waters, from Horbe and Oliveira (2008) in Coruja and Canoas streamwaters, from Neill et al. (2001) in small stream forested and deforested of watersheds 1 and 2 and from Taylor and Mc Lenna (1985) in seawater.

Figure 1

Click here to access/download;Figure;Fig. 1.tif

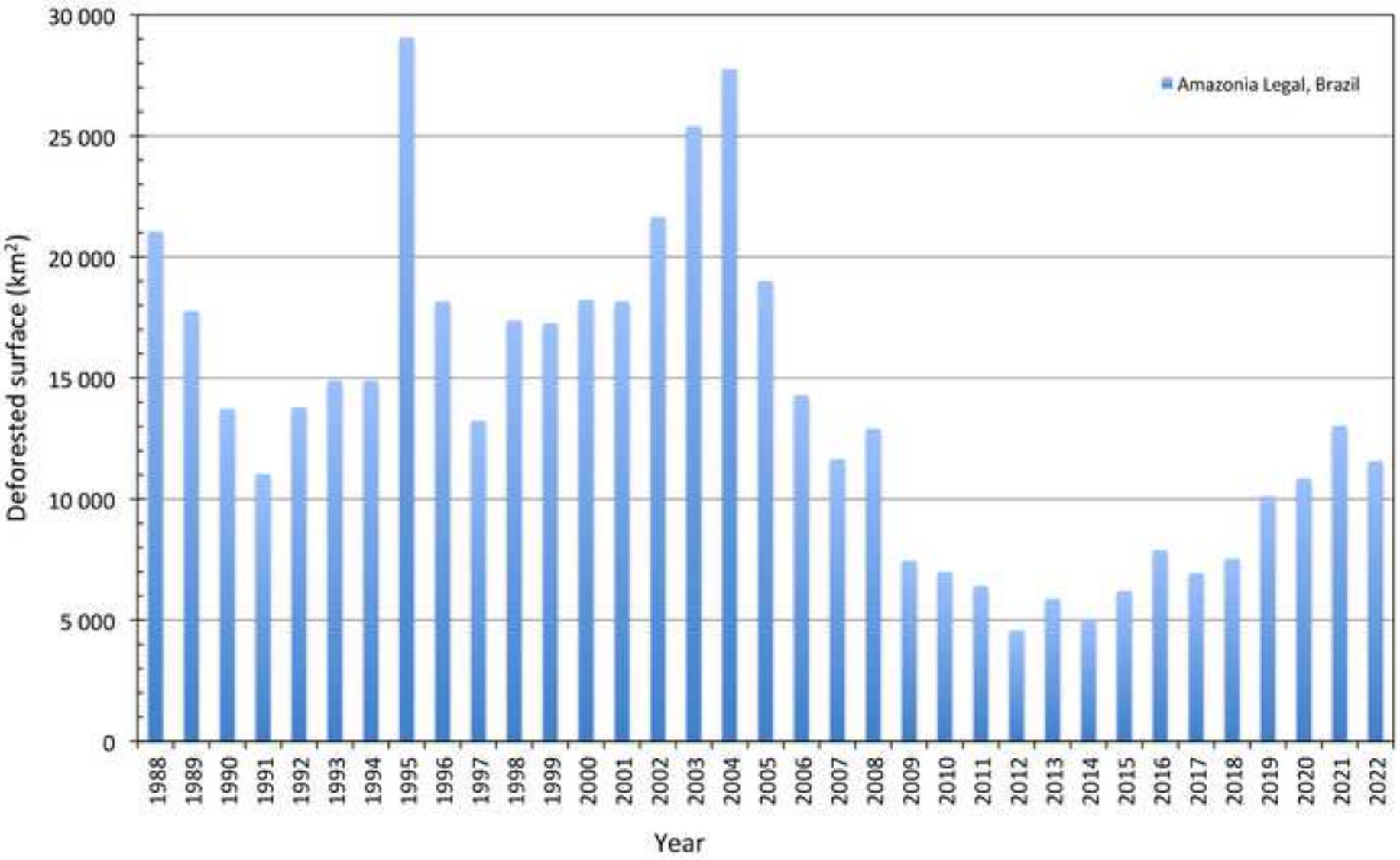

Fig. 1

Fig. 2a

Fig. 2b

Fig. 3a

Fig. 3b

Fig. 3c

Figure 4

Click here to access/download;Figure;Fig. 4.tif

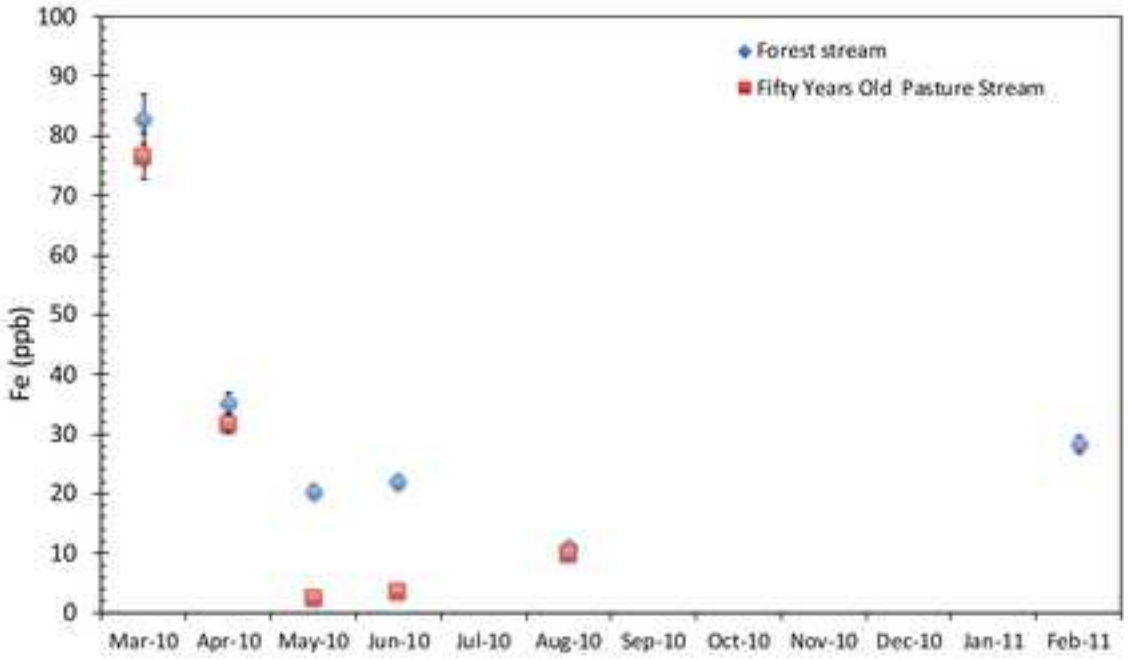

Fig. 4a

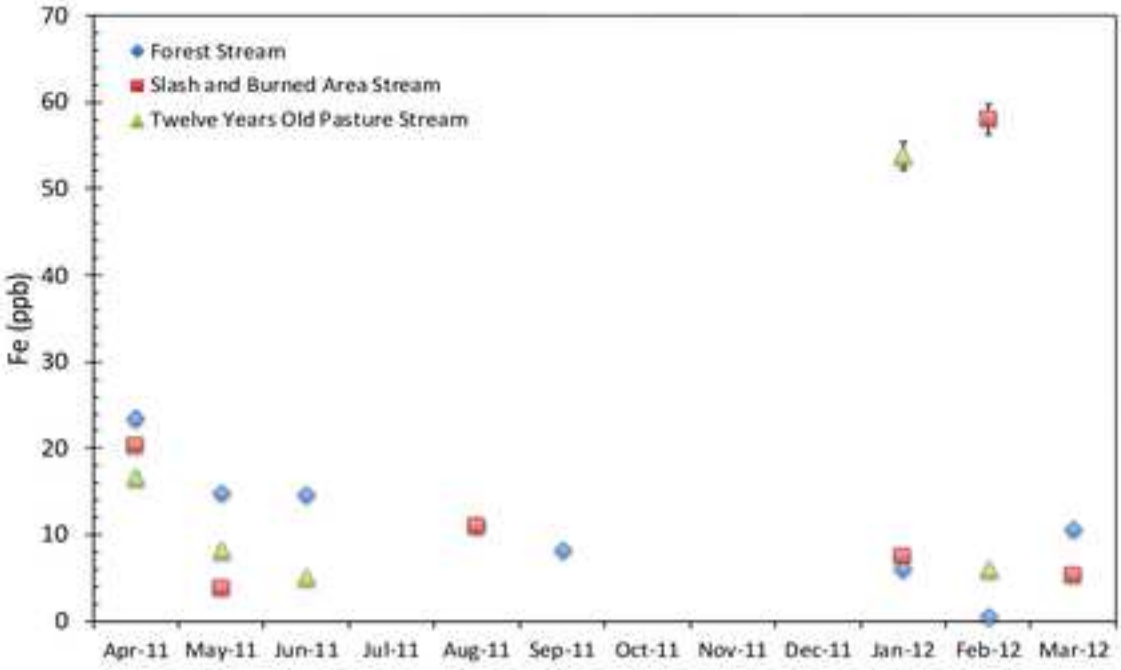

Fig. 4b

Figure 5

Click here to access/download;Figure;Fig. 5.tif

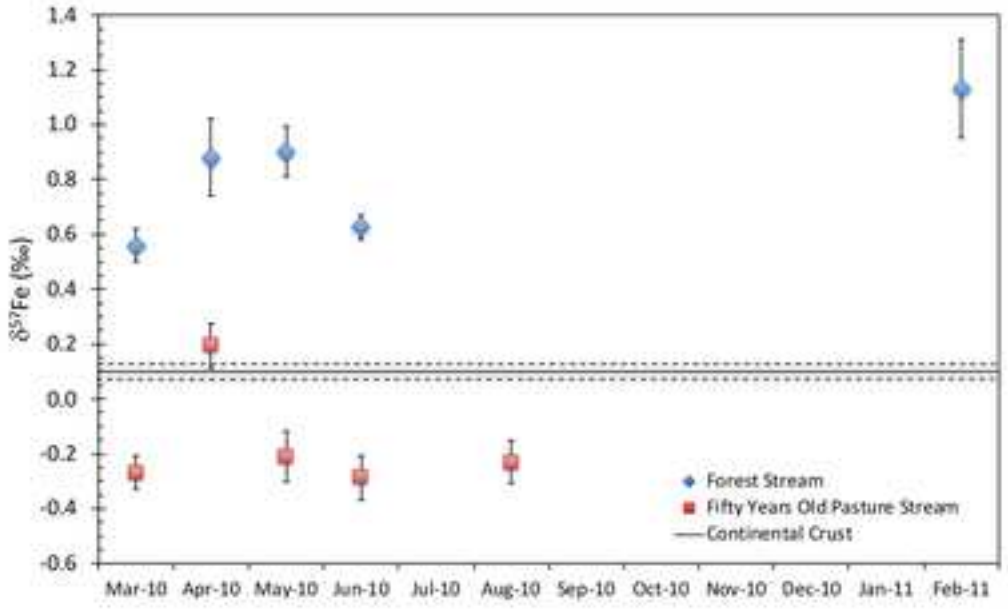

Fig. 5a

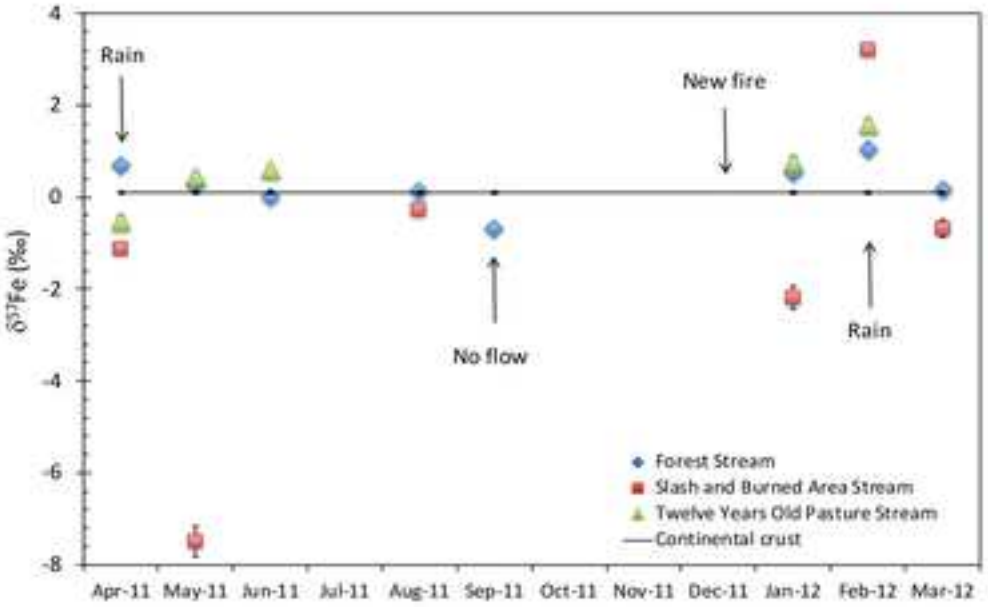

Fig. 5b

Figure 6

Click here to access/download;Figure;Fig. 6 rev.tif

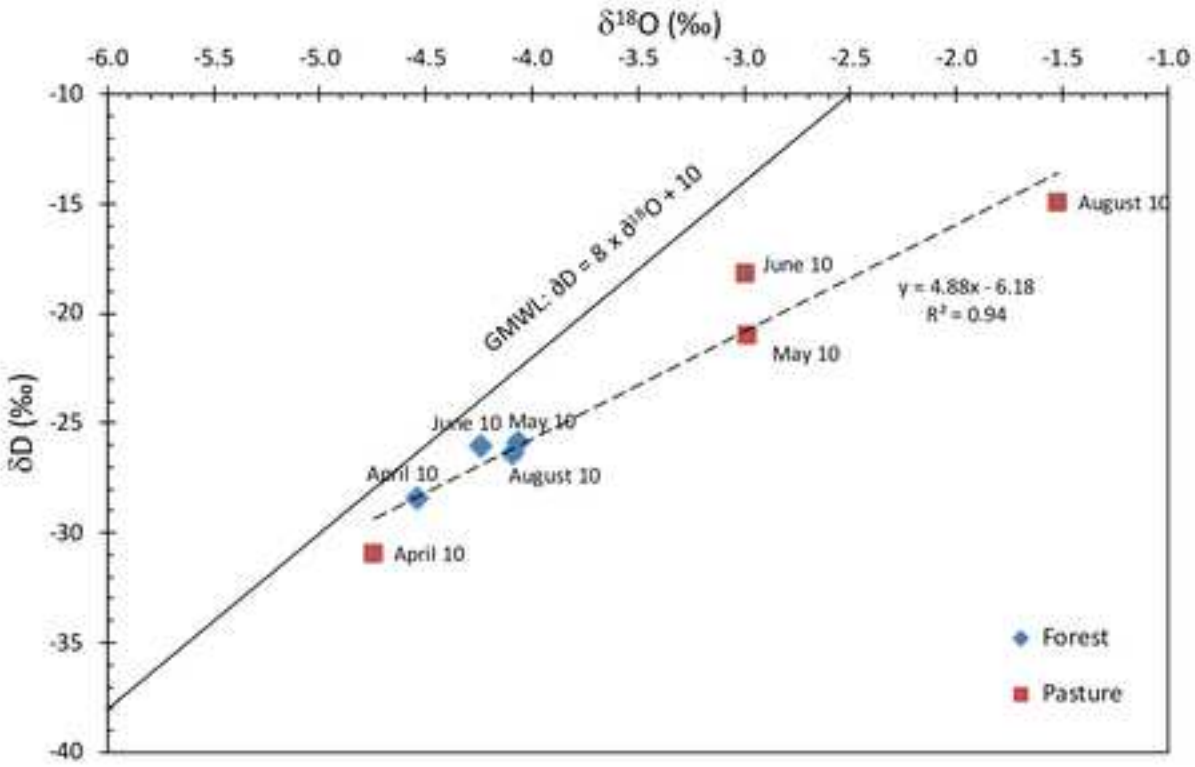

Fig. 6a

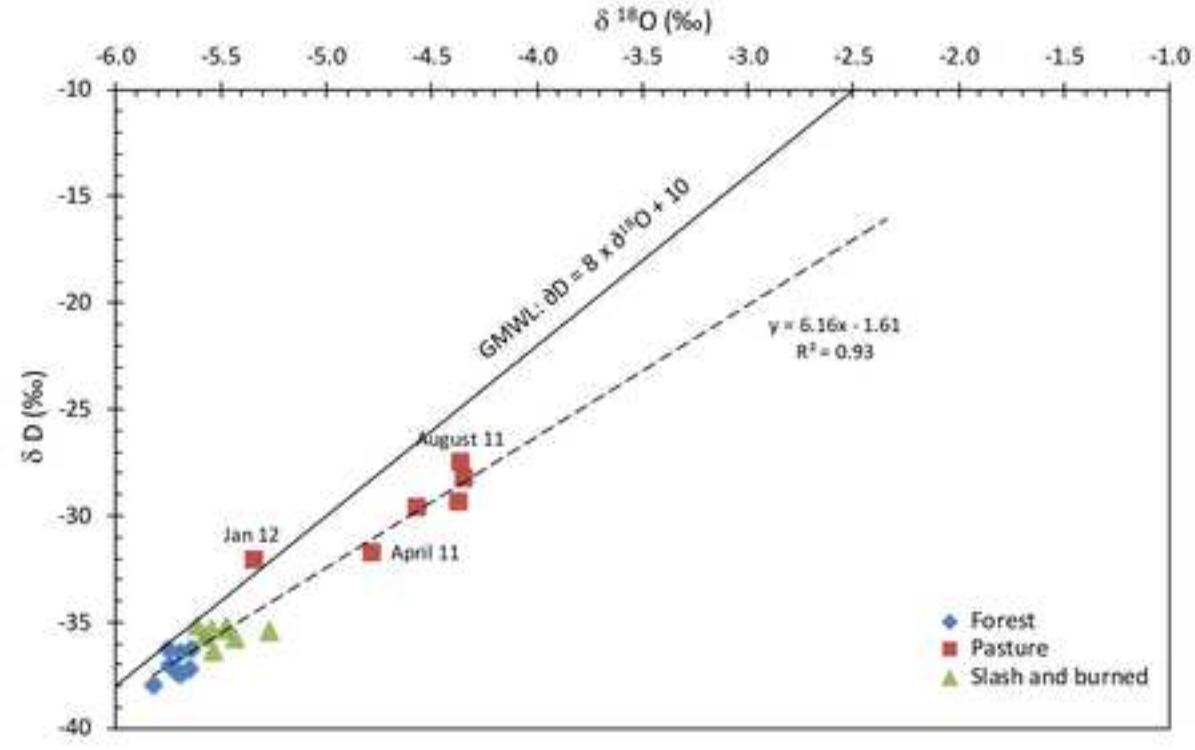

Fig. 6b

Figure 7

Click here to access/download;Figure;Fig. 7.tif

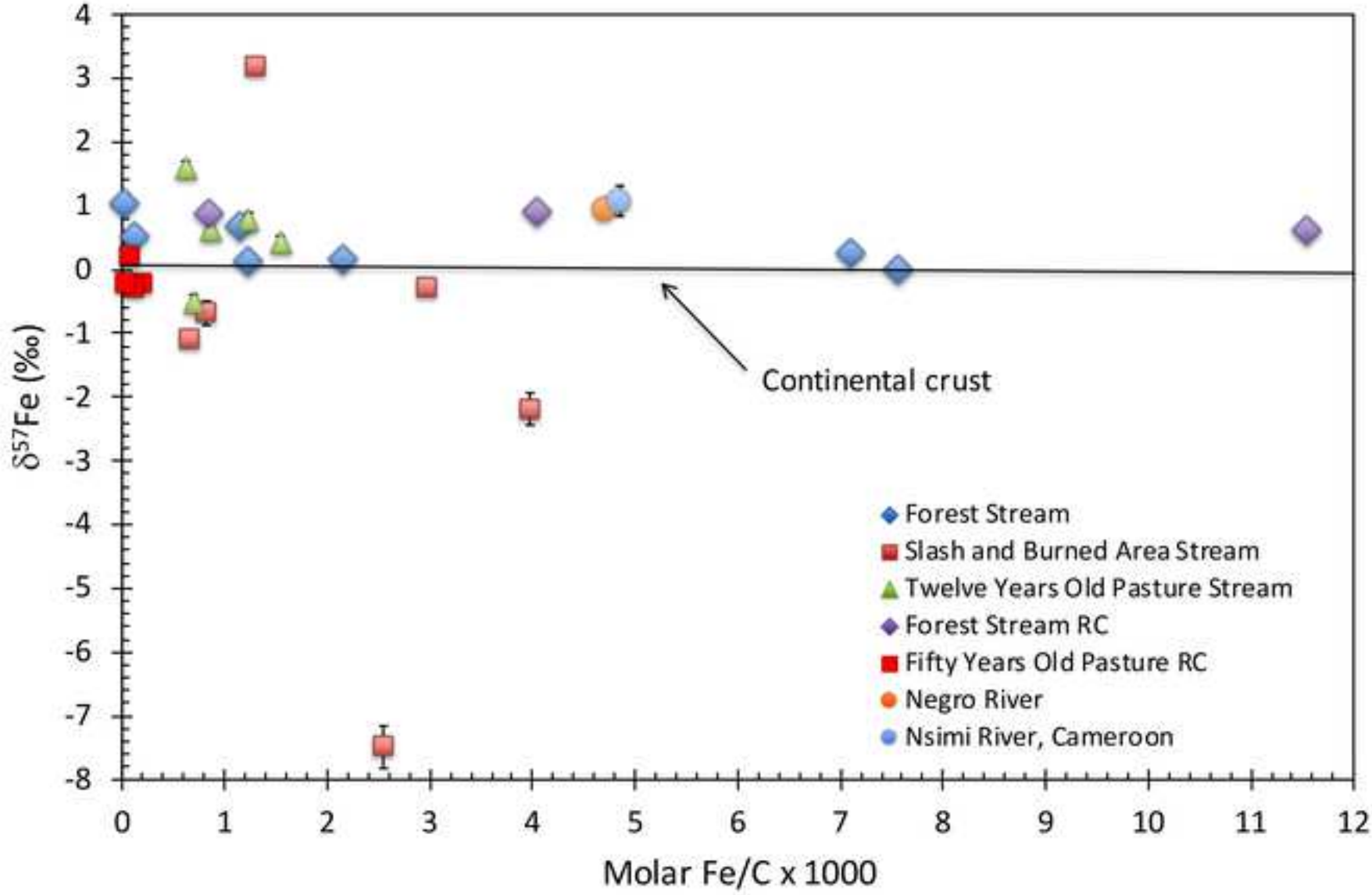

Fig. 7

Table 1: Physical-chemical data and iron isotopic compositions of dissolved stream water samples of the Rio Capim watershed, Para, Brazil.

Sample	Sampling Date	Soil type drained [a]	T°C	pH (± 0.1)	Cond. (µS/cm)	DOC (mg/kg)	[Fe] (µg/kg)	Molar Fe/C x 1000	δ^{57}Fe (‰)	2SE [b]	δ^{56}Fe (‰)	2SE [b]	Number of analyses
Dissolved water samples in forest (F4); S3°46.937', W48°30.711'													
RC1 F4	March 2010 [c]	Albic gleysol	27.0	4.5	12.8	–	82.8	–	0.560	0.060	0.373	0.040	5
RC2 F4	April 2010	Albic gleysol	25.0	4.1	11.1	8.91	35.2	0.85	0.881	0.141	0.587	0.094	3
RC3 F4	May 2010	Albic gleysol	25.5	4.3	15.4	1.09	20.5	4.04	0.902	0.092 [d]	0.601	0.071 [d]	2
RC4 F4	June 2010	Albic gleysol	25.0	3.9	15.7	0.41	22.0	11.5	0.626	0.044	0.417	0.029	3
RC5 F4	August 2010	Albic gleysol	25.4	4.6	16.8	0.76	11.0	3.11	–	–	–	–	
RC7 F4	February 2011	Albic gleysol	25.3	4.7	–	–	28.3	–	1.131	0.179	0.754	0.119	3
Dissolved water samples in 50 years old pasture (P3); S3°45.710', W48°11.239'													
RC1 P3	March 2010 [c]	Gleysol	32.0	6.2	12.2	–	76.6	–	-0.268	0.061	-0.179	0.041	5
RC2 P3	April 2010	Gleysol	30.0	5.2	16.0	11.0	31.8	0.074	0.193	0.081	0.130	0.069	6
RC3 P3	May 2010	Gleysol	33.9	5.2	20.0	2.48	2.59	0.206	-0.210	0.092 [d]	-0.140	0.071 [d]	2
RC4 P3	June 2010	Gleysol	28.5	5.6	19.4	1.91	3.59	0.114	-0.288 [e]	0.081	-0.192	0.064	6
RC5 P3	August 2010	Gleysol	28.1	5.6	19.8	2.10	9.92	0.046	-0.230	0.078	-0.153	0.052	5

[a] See Akerman et al. (2021) for detailed soils description

[b] The iron isotope composition and two standard error uncertainties quoted are calculated from the number of analyses indicated and using the Student's t-correcting factors (Platzner, 1997).

[c] Possible sample storage and filtration artifacts (See text).

[d] Given that only two replicate analyses could be performed, the uncertainty reported are the two standard deviations of the hematite in house standard replicates.

[e] The reported δ^{57}Fe value for this sample was calculated from δ^{56}Fe (δ^{57}Fe as ~1.5 * δ^{56}Fe).

– : No data.

GPS coordinates follow the WGS84 reference frame.

Table 2: Physical-chemical data and iron isotopic compositions of dissolved stream water samples of watersheds near Presidente Figueiredo, Amazonas, Brazil.

Sample	Sampling Date	Soil type drained [a]	T°C	Eh (mV)	pH (± 0.1)	Cond. (µS/cm)	DOC (mg/kg)	[Fe] (µg/kg)	Molar Fe/C x 1000	δ^{57}Fe (‰)	2SE [b]	δ^{56}Fe (‰)	2SE [b]	Number of analyses
Dissolved water samples in forest (F9); S1°42.916', W60°00.710'														
PF1 F9	April 2011	Albic gleysol	25.3	417	5.1	9.0	4.39	23.5	1.15	0.680 [c]	0.079	0.462 [c]	0.046	6
PF2 F9	May 2011	Albic gleysol	26.1	–	5.2	9.0	0.45	14.8	7.11	0.273 [c]	0.034	0.195 [c]	0.032	6
PF3 F9	June 2011	Albic gleysol	25.5	–	4.6	8.0	0.42	14.7	7.56	-0.008 [c]	0.026	0.016 [c]	0.039	6
PF4 F9	August 2011	Albic gleysol	25.6	463	5.1	4.2	1.97	11.2	1.22	0.132 [c]	0.108	0.151 [c]	0.040	6
PF5 F9	September 2011	Albic gleysol	26.6	400	5.3	9.9	–	8.36	–	-0.674	0.102	-0.374	0.033	3
PF8 F9	January 2012	Albic gleysol	26.0	486	5.1	11.0	10.5	6.13	0.13	0.525 [c]	0.111	0.394 [c]	0.041	6
PF9 F9	February 2012	Albic gleysol	24.6	–	4.9	14.0	4.71	0.67	0.03	1.043	0.149	0.713	0.096	3
PF10 F9	March 2012	Albic gleysol	25.4	–	4.8	10.2	1.06	10.6	2.16	0.173 [c]	0.119	0.180 [c]	0.039	6
Dissolved water samples in slash and burned area (P6); S1°42.962', W60°00.574'														
PF1 P6	April 2011	Gleyic Acrisol	27.7	377	5.0	13.5	6.49	20.3	0.67	-1.113 [c]	0.025	-0.746 [c]	0.042	6
PF2 P6	May 2011	Gleyic Acrisol	26.6	–	4.5	9.0	0.33	3.9	2.55	-7.490	0.333	-5.000	0.097	3
PF4 P6	August 2011	Gleyic Acrisol	27.4	379	5.3	9.2	0.79	11	2.98	-0.286	0.062	-0.215	0.018	3
PF5 P6	September 2011	Gleyic Acrisol	29.5	450	5.3	9.9	–	–	–	–	–	–	–	
PF8 P6	January 2012	Gleyic Acrisol	27.5	461	5.2	10.0	0.41	7.6	3.98	-2.186	0.252	-1.376	0.174	3
PF9 P6	February 2012	Gleyic Acrisol	25.6	–	5.7	41.2	9.54	58	1.31	3.193 [c]	0.085	2.138 [c]	0.038	6
PF10 P6	March 2012	Gleyic Acrisol	26.8	–	4.7	12.4	1.41	5.4	0.82	-0.682	0.191	-0.314	0.093	3
Dissolved water samples in 12 years old pasture (P3); S1°47.983', W60°19.276'														
PF1 P3	April 2011	Gleysol	36.0	323	4.9	15.0	5.13	16.6	0.70	-0.520 [c]	0.128	-0.248 [c]	0.075	9
PF2 P3	May 2011	Gleysol	–	–	–	–	1.16	8.3	1.54	0.434 [c]	0.097	0.362 [c]	0.094	6
PF3 P3	June 2011	Gleysol	–	–	–	–	1.29	5.2	0.86	0.606	0.064	0.571	0.055	3
PF4 P3	August 2011	Gleysol	28.5	369	5.1	7.1	11.1	–	–	–	–	–	–	
PF5 P3	September 2011	Gleysol	35.9	382	4.9	30.0	–	–	–	–	–	–	–	
PF8 P3	January 2012	Gleysol	30.0	315	5.5	13.0	9.36	53.8	1.24	0.767 [c]	0.125	0.538 [c]	0.048	6
PF9 P3	February 2012	Gleysol	–	–	–	–	2.11	6.1	0.62	1.584	0.117	1.162	0.116	3

[a] See Akerman et al. (2021) for a detailed soils description

[b] The iron isotope composition and two standard error uncertainties quoted are calculated from the number of analyses indicated and using the Student's t-correcting factors (Platzner, 1997).

[c] Analyses based on two separate sample aliquot mineralization and Fe purification.

– : No data.

GPS coordinates follow the WGS84 reference frame.

Table 3: Hydrogen and oxygen isotope compositions of stream water samples from the Rio Capim watershed, Para, Brazil ("RC" samples) and near Presidente Figueiredo, Amazonas, Brazil ("PF" samples).

Sample	Sampling Date	δD (‰)	$\delta^{18}O$ (‰)
Water samples in forest (F4)			
RC2 F4	April 2010	-28.4	-4.54
RC3 F4	May 2010	-25.8	-4.06
RC4 F4	June 2010	-26.4	-4.09
RC5 F4	August 2010	-26.1	-4.24
Water samples in 50 years old pasture (P3)			
RC2 P3	April 2010	-31.0	-4.74
RC3 P3	May 2010	-18.2	-2.99
RC4 P3	June 2010	-21.0	-2.98
RC5 P3	August 2010	-14.9	-1.52
Water samples in forest (F9)			
PF1 F9	April 2011	-38.0	-5.82
PF2 F9	May 2011	-36.4	-5.69
PF3 F9	June 2011	-37.3	-5.71
PF4 F9	August 2011	-37.0	-5.74
PF5 F9	September 2011	-36.3	-5.64
PF8 F9	January 2012	-36.3	-5.75
PF9 F9	February 2012	-37.2	-5.65
PF10 F9	March 2012	-37.4	-5.69
Water samples in slash and burned area (P6)			
PF1 P6	April 2011	-35.4	-5.27
PF2 P6	May 2011	-35.3	-5.47
PF3 P6	June 2011	-35.7	-5.58
PF4 P6	August 2011	-35.3	-5.54
PF5 P6	September 2011	-35.3	-5.46
PF8 P6	January 2012	-35.2	-5.62
PF8 P6	February 2012	-35.8	-5.44
PF10 P6	March 2012	-36.3	-5.54
Water samples in 12 years old pasture (P3)			
PF1 P3	April 2011	-31.7	-4.78
PF2 P3	May 2011	-29.7	-4.57
PF3 P3	June 2011	-28.3	-4.34
PF4 P3	August 2011	-27.5	-4.36
PF8 P3	January 2012	-32.1	-5.34
PF9 P3	February 2012	-29.4	-4.37

Figure S1

Click here to access/download

Supplementary file

Fig. S1.eps

Figure S2

Click here to access/download

Supplementary file

Fig. S2 rev.tif

Figure S3

Click here to access/download

Supplementary file

Fig. S3 rev.tif

Figure S4

Click here to access/download

Supplementary file

Fig. S4 rev.tif

Figure S5

Click here to access/download

Supplementary file

Fig. S5 rev.tif

Figure S6

Click here to access/download

Supplementary file

Fig. S6 rev.tif